Article

SOURCE DATA | TRANSPARENT PROCESS

EMBO reports

Transcription factor CDF4 promotes leaf senescence and floral organ abscission by regulating abscisic acid and reactive oxygen species pathways in *Arabidopsis*

Peipei Xu*, Haiying Chen & Weiming Cai**

Abstract

Leaf senescence is a highly complex developmental process that is tightly controlled by multiple layers of regulation. Abscisic acid (ABA) and reactive oxygen species (ROS) are two well-known factors that promote leaf senescence. We show here that the transcription factor *CDF4* positively regulates leaf senescence. Constitutive and inducible overexpression of *CDF4* accelerates leaf senescence, while knockdown of *CDF4* delays it. *CDF4* increases endogenous ABA levels by upregulating the transcription of the ABA biosynthesis genes 9-cis-epoxycarotenoid dioxygenase 2, 3 (*NCED2, 3*) and suppresses H_2O_2 scavenging by repressing expression of the catalase2 (*CAT2*) gene. *NCED2, 3* knockout and *CAT2* overexpression partially rescue premature leaf senescence caused by *CDF4* overexpression. We also show that *CDF4* promotes floral organ abscission by activating the polygalacturonase *PGAZAT* gene. Based on these results, we propose that the levels of CDF4, ABA, and ROS undergo a gradual increase driven by their interlinking positive feedback loops during the leaf senescence and floral organ abscission processes.

Keywords ABA biosynthesis; DOF transcription factor; floral organ abscission; leaf senescence; ROS scavenging

Subject Category Plant Biology

DOI 10.15252/embr.201948967 | Received 29 July 2019 | Revised 18 April 2020 | Accepted 30 April 2020 | Published online 2 June 2020

EMBO Reports (2020) 21: e48967

Introduction

Leaf senescence is a very complicated and orderly developmental process that is regulated by age. It involves the degradation of macromolecules and the mobilization and translocation of metabolic products to the younger tissues of the plant [1]. The progression of leaf senescence is regulated not only by many internal factors, such as the reproductive status of the plant, metabolism, and transcriptional regulators, but also by various stresses [2,3]. Its initiation, progression, and completion are tightly regulated by multiple layers of regulatory factors. Plant hormones play a key role in controlling the progression of leaf senescence. Cytokinins (CK) [4,5] and gibberellic acid (GA) [4,6], together with auxins [7], are thought to be senescence-suppressing hormones, while ethylene (ETH), jasmonic acid (JA), salicylic acid (SA), and abscisic acid (ABA) are thought to be senescence-promoting factors. ETH is a well-known hormonal regulator of leaf senescence, and mutations that affect ETH biosynthesis or signaling alter the progression of leaf senescence [8,9]. In *Arabidopsis thaliana*, senescing leaves have higher concentrations of ABA and SA than non-senescing leaves [10]. In senescing *Arabidopsis* leaves, many ABA and SA biosynthesis-related genes are upregulated [11].

ABA is a sesquiterpenoid, and its biosynthetic genes have been cloned [12]. The NCEDs (9-*cis*-epoxycarotenoid dioxygenases) function in the cleavage of xanthophylls and are rate-limiting enzymes that regulate ABA biosynthesis [13]. ABA DEFICIENT 3 (ABA3) is involved in the synthesis of the molybdenum co-factor that is needed for NCED3 activity [14]. ABA plays important roles not only in the response to abiotic stress but also in seed dormancy, abscission, and senescence [12]. Previous reports have shown that exogenous ABA treatment induces senescence and strongly upregulates senescence-associated genes (SAGs), but the molecular mechanisms underlying this effect are not well characterized. One of the ABA regulators during senescence is the NAC transcription factor, NAC-like, activated by AP3/P1 (NAP), which was shown to control expression of ABA biosynthesis genes [15]. ATAF1 was shown to regulate *NCED3* [16]. In addition, many ABA metabolism- and signaling-related genes have roles in controlling senescence [17]. The ABA receptor PYL9 positively regulates leaf senescence and improves plant drought tolerance [18].

Drought, salinity, high light levels, high temperature, and some important developmental changes can promote endogenous H_2O_2 accumulation, which is responsible for an accelerated leaf

Laboratory of Photosynthesis and Environment, CAS Center for Excellence in Molecular Plant Sciences, Shanghai Institute of Plant Physiology and Ecology, Chinese Academy of Sciences, Shanghai, China
*Corresponding author. Tel: +86 021 54924249; E-mail: ppxu@sibs.ac.cn
**Corresponding author. Tel: +86 021 54924248; E-mail: wmcai@sibs.ac.cn

senescence process. Increased protein and lipid oxidation caused by upregulated H_2O_2 levels are characteristics of senescence-associated syndrome [19]. The *Arabidopsis jub1* (*JUNGBRUNNEN 1*) and *cpr5* (CONSTITUTIVE EXPRESSION OF PR GENES) mutants exhibit an early-leaf-senescence phenotype because of the accumulation of excessive amounts of H_2O_2 [20,21]. However, the *ntl4* (*NAC WITH TRANSMEMBRANE MOTIF 1-LIKE4*) mutant, with downregulated H_2O_2 accumulation, shows delayed drought-related leaf senescence [22]. In addition, the functional relationship between ABA and ROS in leaf senescence has previously been reported in many studies. For example, ROS has been proposed to function as a second messenger in ABA signaling in guard cells [23]. Mutations in the NADPH oxidase catalytic subunit genes *AtRBOHD* and *AtRBOHF* impair ABA-induced stomatal closure and ABA-induced cytosolic Ca^{2+} increases in guard cells [24]. ABA is capable of increasing H_2O_2 levels in maize embryos and seedlings, further supporting the roles of ROS in ABA signaling [25].

Although regulation of leaf senescence in plants is important, the underlying molecular mechanisms are not fully understood. Many methods have been used to isolate a series of SAGs with altered transcript levels in senescing leaves [26]. Transcriptome analyses have shown that hundreds of genes are specifically induced during age-related leaf senescence [27]. Furthermore, many plant-specific transcription factors can regulate these SAGs [28]. However, knockdown mutants of relatively few of these transcription factors produce altered leaf senescence phenotypes. For instance, *AtWRKY53* is strongly upregulated early in leaf senescence, and its knockdown mutant is defective with respect to age-related senescence [29]. *AtWRKY6* expression is induced by leaf senescence [30]. Mutations of the genes encoding NAC transcription factors NAP or ORS1 (Oresara 1 sister 1) delay leaf senescence [31,32]. *EIN3* accelerates leaf senescence by repressing transcription of the microRNA miR164 [33]. *ORE1* (*Oresara 1*) regulates the leaf senescence process in the trifurcate feed-forward pathway [34]. *VNI2* integrates abscisic acid signals with leaf senescence via the *COR/RD* genes [35]. *JUB1* negatively regulates leaf senescence [36], and *NAC016* overexpression also induces leaf senescence [37]. Environmental stimuli induce the transcriptional regulators PIF4 and PIF5, which also promote dark-induced senescence by inducing *ORE1* expression [38].

Organ abscission is a typical cell separation process that occurs throughout the plant's growth cycle [39]. At the predetermined abscission position, an abscission zone (AZ) develops. The AZ cells recognize abscission signals that activate cell wall-loosening proteins. Endoglucanases, polygalacturonases, and expansins have been well documented as the cell wall-loosening proteins [40,41]. Many genes have been found to be involved in the regulation of organ abscission. The *ida* mutant has a delayed abscission phenotype [42], and the HAESA and HAESA-LIKE2 receptor-like kinases are activated by interactions with INFLORESCENCE DEFICIENT IN ABSCISSION (IDA) [43]. Moreover, the transcription factors AGL15, DOF4.7, and ZFP2 are involved in the regulation of the floral organ abscission process [44–46].

The DNA-binding with one finger (DOF) family proteins have been reported to participate in many biological processes since the first DOF transcription factor, ZmDOF1, was found to be a light-response factor in maize [47]. *Arabidopsis* DOF proteins have been shown to function in many developmental processes, such as flowering time, leaf prioritization, light response, cell cycle progression, secondary metabolism, nitrate response, inter-fascicular cambium formation, and root development [46,48–58]. By screening the DOF protein family, we identified the leaf senescence-related transcription factor *CDF4*. Induced or constitutive overexpression of *CDF4* promoted leaf senescence, while delayed leaf senescence was observed in transgenic plants in which *CDF4* expression was downregulated. Furthermore, CDF4 controlled the endogenous ABA level and H_2O_2 scavenging by positively regulating the transcription of genes involved in ABA biosynthesis and by repressing catalase activity. Genetic analysis showed that CDF4-induced ABA biosynthesis and H_2O_2 accumulation are critical for accelerating the progression of leaf senescence. We also found that *CDF4* promotes floral organ abscission by regulating expression of the *PGAZAT* polygalacturonase gene. This study discovers a novel tripartite amplification loop, involving *CDF4*, ABA, and ROS, which are mutually promoted by distinct mechanisms, and provides insights into the molecular regulatory network of leaf senescence and floral organ abscission in *Arabidopsis*.

Results

The *CDF4* gene encodes a leaf senescence-related transcription factor

To uncover the genetic network behind the transcriptional regulation of leaf senescence, we systematically screened genes belonging to the plant-specific DOF transcription factor family in *Arabidopsis*. We used real-time quantitative PCR (qPCR) to quantify transcript abundance of the subfamily of DOF A, B, D, E family genes in *Arabidopsis* rosette leaves at different developmental stages (Appendix Fig S1A). Interestingly, the cycling DOF family gene *CDF1-5* expression patterns were age-dependent (Appendix Fig S1B and C). The cycling DOF family genes were previously implicated in photomorphogenesis [59]. Among the family members, *CDF4* (AT2G34140) is of particular interest because changing its expression level, but not that of any other cycling DOF family gene, can affect leaf senescence [58,60–62]. CDF4 exhibited similarities with CDF1, CDF2, CDF3, and CDF5 in terms of amino acid (aa) sequence (Appendix Fig S2). CDF4 was previously reported to be a nucleus-localized transcription factor [63]. As with the other nucleus-localized DOF transcription factors, the 171-aa CDF4 protein had a DNA-binding domain at the N-terminus (Fig 1A).

We wanted to determine whether the DOF family protein CDF4 has transcriptional activity. The DNA-binding domain was at the N-terminus of CDF4, which suggested that the C-terminal sequence of CDF4 was critical for its transcriptional activity. Compared with expression of the vector control, expression of the *CDF4* sequence repressed luciferase activity by approximately 74%, indicating that CDF4 was a transcriptional repressor. To examine its transcriptional regulatory domain in detail, we obtained a series of *CDF4* coding sequence deletions, fused them to the GAL4 DNA-binding domain (Fig 1B, left panel), and co-transformed them into *Arabidopsis* protoplasts with a reporter vector. The negative control had no luciferase activity. The sequence consisting of residues 61–171, without the N-terminal region compromised transcriptional repression by CDF4 in our assay. However, transcriptional activation activity was

detected in the C-terminal region consisting of aa residues 111–171 or 121–171, and expression of this region upregulated luciferase activity by 1.3- to 1.8-fold. But the sequence consisting of aa residues 1–110 repressed luciferase activity by 88%. The N-terminal region, including the DOF domain, somehow inhibited the trans-activation activity of CDF4 (Fig 1B, right panel). These results

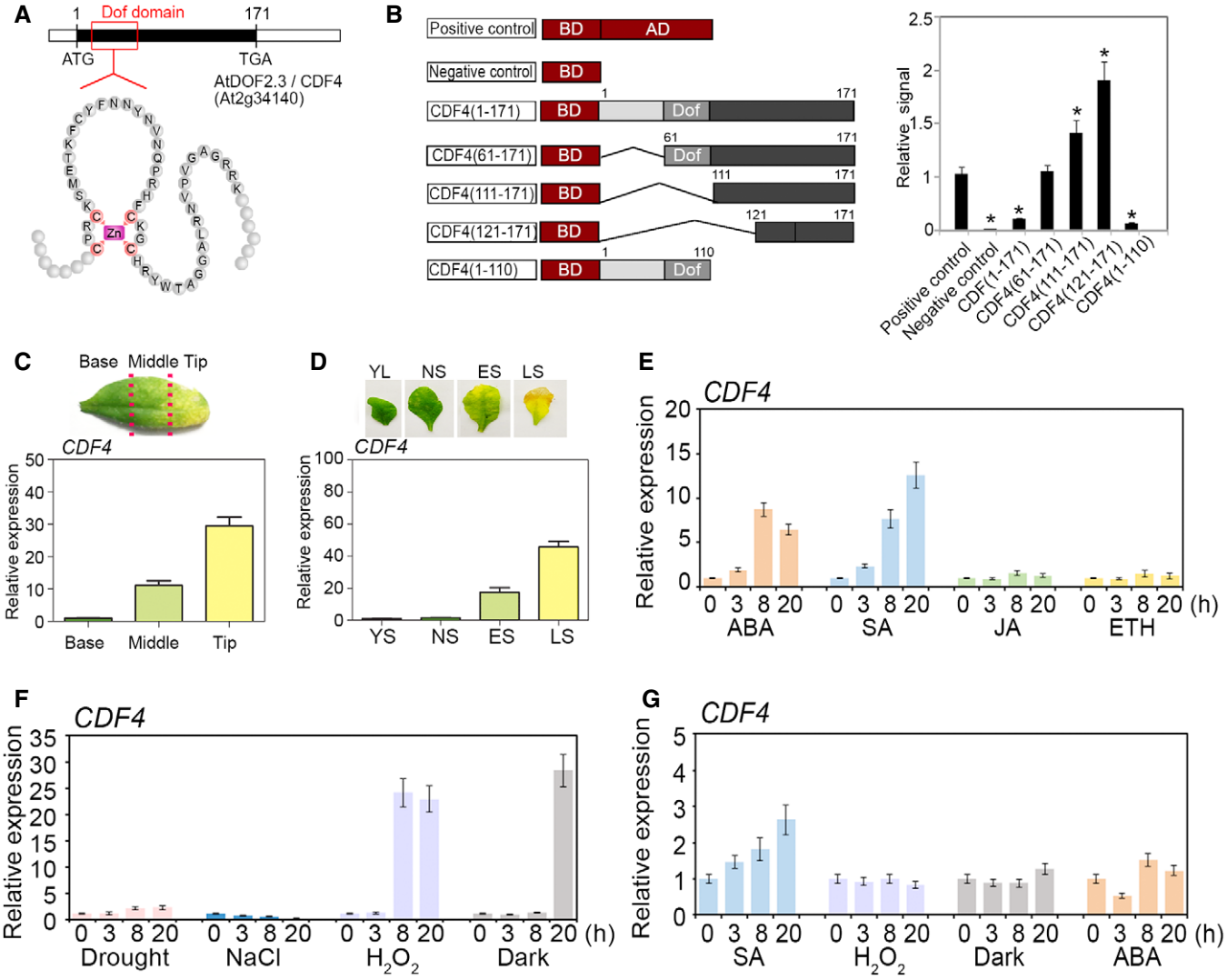

Figure 1. Molecular characterization of the *CDF4* gene and effects of ABA, SA, H_2O_2, abiotic stresses and darkness on its expression in *Arabidopsis* leaves.

A The gene and protein structures of the DOF domain of CDF4. Cysteine residues conserved in the DOF domain are indicated in red, and the conserved DOF Zn-figure DNA-binding domain is found in CDF4.

B *Trans*-activation activity assays of CDF4 in *Arabidopsis* protoplasts. The full-length ORF of *CDF4* and its four deletion constructs are described in the Methods section. DOF (gray boxes) represents the DNA-binding domains of CDF4. Negative control was the effector vector without gene inserts. The effector vector used is shown in the left panel. The *GAL4* transient expression assays were performed using *Arabidopsis* protoplasts, shown in the right panel. Deletion of the CDF4 N-terminal domain compromised the transcriptional repression by *CDF4* in our assay. Three independent experiments were conducted. Values are given as mean ± SD, $n = 3$. $^*P < 0.05$ by Student's *t*-test.

C Localized expression of *CDF4* in a senescing rosette leaf. The ~ 50% senesced rosette leaf was cut into three parts as indicated by the red lines. The level of *CDF4* mRNA was determined in the three sections of the senescing leaf: base; middle; and tip. Three independent experiments were conducted. Values are given as mean ± SD, $n = 3$.

D *CDF4* expression level at various developmental stages of rosette leaves: YL, young leaf; NS, fully expanded, non-senescent leaf; ES, early-senescent leaf, with 1/4 leaf area turned yellow; and LS, late-senescent leaf, with > 50% leaf area turned yellow. Three independent experiments were conducted. Values are given as mean ± SD, $n = 3$.

E Effect of plant growth hormones (1 mM SA, 1 μM ABA, 10 μM JA, and 10 μM 1-aminocyclopropane -1-carboxylic acid (ACC)) on *CDF4* expression. Three independent experiments were conducted. Values are given as mean ± SD, $n = 3$.

F Effects of abiotic stress treatments on *CDF4* expression. Rosette leaves were treated with salt (100 mM NaCl), drought, H_2O_2 (2 mM), or darkness. Three independent experiments were conducted. Values are given as mean ± SD, $n = 3$.

G Effects of SA, H_2O_2, and dark treatment on *CDF4* expression in the *aba2-1* mutant background. *AtACT2* was used as an internal control. Three independent experiments were conducted. Values are given as mean ± SD, $n = 3$.

showed that CDF4 was a senescence-related functional transcription factor. Similarly, maize DOF2 and barley PBF could act as either activators or repressors, depending on the downstream promoter or interaction partners [47].

CDF4 transcript levels increase as leaves age and are regulated by dark and H_2O_2 treatments

To identify the role played by *CDF4* in developmental processes, we used qPCR to check the *CDF4* mRNA level in leaves at different developmental stages. When *Arabidopsis* rosette leaves displaying ~ 50% senescence were cut into three parts along the leaf axis (basal, middle, and tip; Fig 1C, top panel), the *CDF4* transcript was detected at a low level in the basal part of the leaf, but was highly abundant in the leaf tip (Fig 1C). *CDF4* mRNA levels were low in younger leaves but were more abundant at later stages when leaves were senescing (Fig 1D). Analysis of rosette leaves of pro*CDF4*::GUS plants at the early-senescence stage detected GUS signals in the leaf tip (Appendix Fig S3D). These results indicated that *CDF4* expression is developmentally associated with leaf senescence. Therefore, we characterized the temporal and spatial expression patterns of *CDF4*. RNA samples obtained from various organs indicated that *CDF4* was expressed at a relatively high level in the root, silique, and flower (Appendix Fig S4A).

To assess whether environmental cues affect *CDF4* expression, we determined the effect of plant hormones and various environmental treatments on the *CDF4* mRNA level in rosette leaves. The results showed that *CDF4* expression was upregulated by ABA and SA treatments but was not affected by JA or ETH (Fig 1E). Twenty hours of dark treatment upregulated the *CDF4* gene expression approximately 20-fold, but salt and drought treatments did not affect *CDF4* expression (Fig 1F). H_2O_2 has key roles in *Arabidopsis* stress responses, and abiotic stress results in the accumulation of endogenous H_2O_2. We confirmed that *CDF4* expression responded positively to H_2O_2 treatment in *Arabidopsis* seedlings (Fig 1F). The effects of SA, H_2O_2 and dark treatments on *CDF4* expression in the ABA-deficient *aba2-1* mutant were analyzed to determine whether the induction of *CDF4* relies on ABA [64] (Fig 1G). The results indicated that *CDF4* expression was reduced significantly in the *aba2-1* mutant background. Therefore, the *CDF4* gene is regulated by SA, H_2O_2, and dark treatments in a partly ABA-dependent manner.

Leaf senescence is accelerated in *CDF4*-overexpressing transgenic lines

To identify the potential role of CDF4 in the control of leaf senescence, we generated transgenic lines that constitutively overexpressed *CDF4* under the control of the CaMV 35S promoter (Fig 2A). *CDF4* overexpression in 35S::*CDF4* transgenic lines was verified by qPCR (Appendix Fig S5A and B). Analysis of leaf longevity showed that the transgenic plants constitutively expressing *CDF4* had an accelerated leaf senescence phenotype compared with the vector control, but the leaf senescence process was not different between wild-type Col-0 and the vector control plants (Appendix Fig S6). We propose that the phenotype of the 35S::*CDF4* plants results from *CDF4* promotion of the senescence program. Many genes, including *SAG12*, which encodes a cysteine protease, and *SAG13*, which encodes a short-chain alcohol dehydrogenase, are known to be induced during developmentally related senescence. Therefore, we assayed *SAG12* and *SAG13* expression in the 35S::*CDF4* transgenic plants. *SAG12* was expressed at more than a 900-fold higher level, whereas *SAG13* expression was increased 50-fold in 35S::*CDF4* plants (Fig 2B). The upregulation of *SAG12* and *SAG13* verified that the phenotype of 35S::*CDF4* was due to activation of the senescence program. The 35S::*CDF4* transgenic plants were smaller than the vector control plants (Appendix Fig S5A and D), potentially due to reduced cell size (Appendix Fig S5C and F). It was interesting that constitutive overexpression of many DOF family transcription factor genes, such as *OBP1*, *OBP2*, *OBP3*, *OBP4*, *AtDOF5.1*, *HCA2/AtDOF5.6*, *SCAP1/AtDOF5.7*, and including *CDF4*, can cause plant dwarfing, although the other biological functions of these genes in plant growth and development are diverse [48,50,51,53–55]. We determined the expression levels of cell expansion-related factor genes, and the results showed that many of them were downregulated in 35S::*CDF4* transgenic plants (Appendix Fig S5G). The possible explanation is that these DOF transcription factors conservatively inhibited the expression of cell wall elongation factors and thus inhibited cell expansion. Taken together, we showed that the senescence-related pathways were promoted in plants in which *CDF4* was constitutively overexpressed, and cell expansion was inhibited.

Perturbation of plant homeostasis could result in an early-senescence phenotype. Thus, the early senescence observed in 35S::*CDF4* transgenic plants could indirectly result from general physiological and/or metabolic disturbances. To rule out general metabolic perturbation due to constitutive overexpression of *CDF4*, transgenic plants of *CDF4* gene under the control of an estradiol-inducible promoter were obtained. RT–qPCR indicated that *CDF4* expression in the transgenic plant was clearly induced by estradiol treatment (Appendix Fig S7). Whole plants were sprayed daily with estradiol for 1 week at 18 days after planting, and the effect of inducing *CDF4* overexpression on the leaf senescence process was investigated. Estradiol treatment caused early leaf yellowing and reduced chlorophyll concentration in the transgenic plants with inducible *CDF4* (Fig 2C and D). Furthermore, inducible overexpression of *CDF4* in the young seedlings led to a stunted growth phenotype and obvious downregulation of the lateral root number (Appendix Fig S8). Thus, we concluded that temporary activation of overexpression of *CDF4* promoted leaf senescence. H_2O_2 treatment is thought to cause leaf senescence. The accelerated leaf senescence phenotype of the inducible *CDF4*-overexpressing plants was also assessed in response to H_2O_2 treatment under darkness. Leaves of the transgenic estradiol -induced *CDF4*-overexpressing plants became more yellowish than the leaves of the vector control plant after 3 days in the dark (Fig 2E). Measurements of chlorophyll concentration indicated that leaves of the estradiol-treated inducible *CDF4* transgenic plants had less chlorophyll than did those of the vector control plants (Fig 2F). These data demonstrated that *CDF4*-overexpression was sufficient to induce early leaf senescence.

Knockdown of *CDF4* delays natural and H_2O_2-induced leaf senescence

No T-DNA insertion mutants for *CDF4* were available in the public seed collections. Therefore, in order to continue to investigate *CDF4* molecular functions in controlling senescence, we generated *CDF4* RNA interference (RNAi) knockdown transgenic lines. RNAi

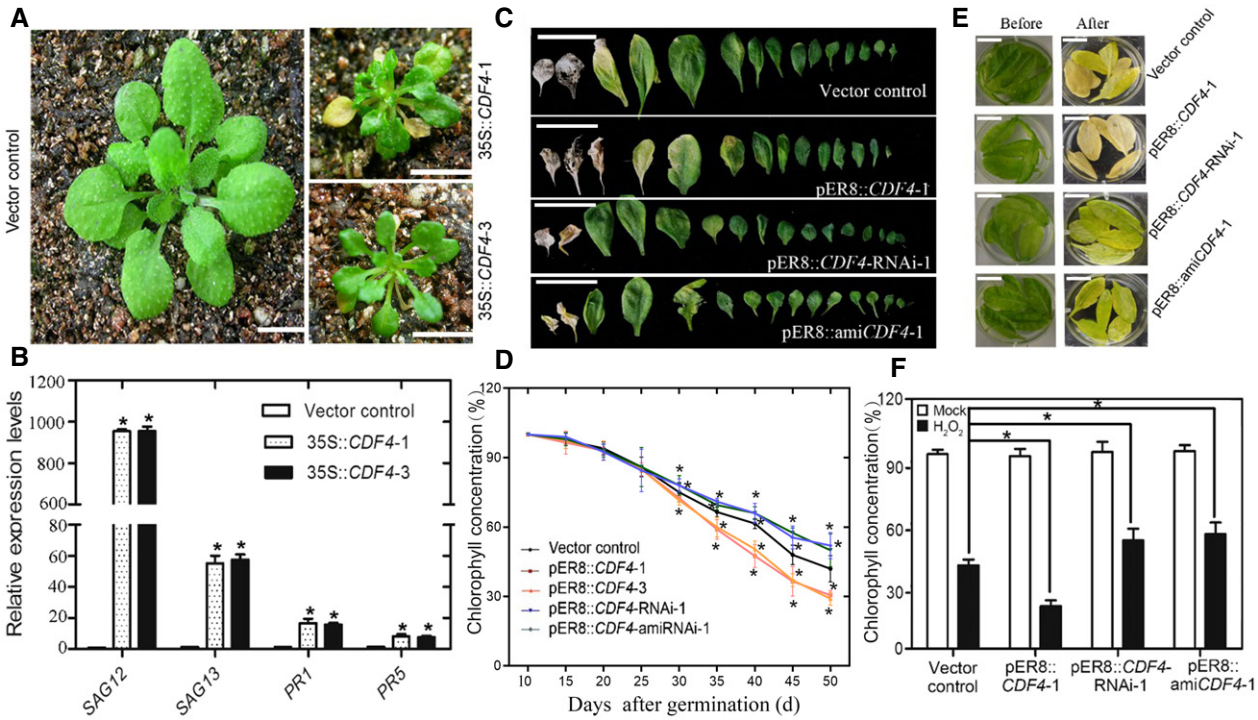

Figure 2. Overexpression or knockdown of *CDF4* in transgenic plants affects leaf senescence.

A The age-dependent leaf senescence symptoms in the vector control and 35S::*CDF4* lines grown under long-day conditions were shown at 21 days old. The 35S::*CDF4* plants had a small leaf size and extremely early-leaf-senescent phenotype, while the control vector leaves were fully green. Scale bars indicate 1 cm.

B The increase in *SAG12*, *SAG13*, *PR1*, and *PR5* gene expression levels was investigated in 35S::*CDF4* plants. Three independent experiments were conducted. Values are given as mean ± SD, $n = 3$. *$P < 0.05$ in comparison with the vector control by Student's *t*-test.

C Phenotypes of vector control, pER8::*CDF4*, pER8::*CDF4*-RNAi, and pER8::ami*CDF4* plants, after treatment with 20 μM estradiol for 7 days at 18 days old. Scale bars indicate 1.5 cm.

D The leaf senescence phenotypes of detached rosette leaves in vector control, pER8::*CDF4*, pER8::*CDF4*-RNAi, and pER8::ami*CDF4* lines before and after treatment with 2 mM H_2O_2 in the dark for 4 days. Scale bars indicate 0.7 cm.

E Analysis of the relative chlorophyll concentration in the sixth and seventh rosette leaves from the vector control, pER8::*CDF4*, pER8::*CDF4*-RNAi, and pER8::ami*CDF4* lines shown at various development stages. Four independent experiments were conducted. Values are given as mean ± SD, $n = 4$. *$P < 0.05$ by Student's *t*-test.

F The chlorophyll concentration in leaves from (D) was analyzed. The percentage indicates the chlorophyll content relative to vector control before treatment. Four independent experiments were conducted. Values are given as mean ± SD, $n = 4$. *$P < 0.05$ by Student's *t*-test.

Source data are available online for this figure.

transgenic lines with a high *CDF4* repression level were utilized in the subsequent assays (Appendix Fig S7A). Due to the sequence similarity of DOF transcription factors, the specificity of RNAi in our assay was checked as well; the knockdown transgenic lines did not exhibit any significant change in the gene expression of the COG1 genes (Appendix Fig S7B). Compared with the vector control, leaf senescence was delayed in the pER8::*CDF4*-RNAi transgenic lines following estradiol treatment (Fig 2C). When the vector control plants had brownish dead leaves, most of the leaves on the pER8::*CDF4*-RNAi plants remained green. Consistent with this phenotype, we found that chlorophyll concentration declined to 60% of that in the vector control lines at 40 days after planting, and similar chlorophyll losses occurred at 44 days after planting in the pER8::*CDF4*-RNAi plants (Fig 2D). In addition, inducible inhibition of *CDF4* expression in 7-day-old seedlings promoted plant development, with an increased lateral root number (Appendix Fig S8A and B). We also used the artificial microRNA (amiRNA) gene silencing method to obtain pER8::ami*CDF4* transgenic lines with a high *CDF4* repression level. Compared with the wild-type control, leaf senescence was delayed in pER8::ami*CDF4* plants in response to estradiol treatment (Fig 2C). Previous research has shown that natural and dark-induced leaf senescence overlap considerably in terms of cellular processes and molecular mechanisms [28]. We found that H_2O_2, ABA, and dark-induced leaf senescence were delayed in both pER8::*CDF4*-RNAi and pER8::ami*CDF4* plants (Fig 2E and Appendix Fig S8C). Consistent with this delayed senescence phenotype; chlorophyll loss was also delayed (Fig 2F). Furthermore, we found that ABA treatment partially restored the leaf senescence phenotype of *CDF4* knockdown plants (Appendix Fig S9). And exogenous fluridone (ABA biosynthesis inhibitor) or ROS generation inhibitor DPI (diphenyleneiodonium) treatments delayed the leaf senescence phenotype of *CDF4*-overexpressing plants (Appendix Fig S9). In addition, we obtained two mutants, CS91480 and CS87649, from the Nottingham Arabidopsis Stock Centre (NASC) mutant repository and found that each of them had a single amino acid substitution, at the 90 and 105aa positions, respectively, of the conserved DOF

domain (Appendix Fig S10A). Compared with the wild-type control, leaf senescence was delayed in both mutants (Appendix Fig S10B). Furthermore, phenotypic complementary test showed that the wild-type CDF4 genomic DNA can complement the leaf senescence phenotype of the mutants. These results confirm the function of *CDF4* in promoting leaf senescence.

CDF4 promotes ABA biosynthesis by inducing the transcription of *NCED2* and *NCED3*

A previous research demonstrated that an atypical bipartite NLS with a 17 amino acid long linker between its flanking basic regions directs *Arabidopsis thaliana* DOF proteins to the cell nucleus [65]. As expected, CDF4 proved to be a nuclear protein (Appendix Fig S4B). Next, we sought to explore how *CDF4* promotes leaf senescence. To test whether endogenous hormone levels were altered in *CDF4* transgenic plants, we first determined the ABA concentration in the vector control, *CDF4*-overexpressing and *CDF4*-repressing plants. In pER8::*CDF4* leaves, the ABA concentration increased from 0.342 nmol/g fresh weight (FW) to 0.612 nmol/g FW and 0.576 nmol/g FW (fresh weight) (FW) over 3 days of treatment with estradiol, but the ABA levels in the pER8::*CDF4*-RNAi plants decreased by approximately 60% after 4 days of estradiol treatment (Fig 3A). These results indicated that the *CDF4* gene regulated endogenous ABA levels in *Arabidopsis*. To investigate the mechanisms underlying the function of *CDF4* in ABA biosynthesis and leaf longevity, we searched for ABA biosynthesis- and signaling-related genes which exhibited altered mRNA levels in *CDF4*-overexpressing or knockdown transgenic lines; among these genes, we found that *NCED2*, *NCED3*, *NCED6*, *AAO2*, *AAO3,* and *CYP707A1* were highly upregulated in the 35S::*CDF4* lines (Fig 3B and C). However, the selected SA biosynthesis- and signaling-related genes were not significantly altered in 35S::*CDF4* lines (Appendix Fig S11A). Additionally, only *NCED2* and *NCED3* were clearly downregulated in the *CDF4* knockdown transgenic plants (Appendix Fig S11B). The expression of the *NCED* family genes has been reported to increase in senescing leaves [26]. Another *Arabidopsis* aldehyde oxidase (AAO) family gene, *AAO3,* is targeted by NAP, which promotes ABA accumulation and leaf senescence in *Arabidopsis* [59]. By using the glucocorticoid-mediated transcriptional induction system in transgenic plants, we wanted to determine whether *NCED2* and *NCED3* were immediately downstream of *CDF4*. And their expressions were induced in the *CDF4*GR transgenic plants after dexamethasone (DEX) induction in the absent or presence of cycloheximide (CHX) (Fig 3D–G). The DEX induction assays suggested that *NCED2* and/or *NCED3* were likely downstream targets of CDF4, which contributed to the altered ABA level in *CDF4* transgenic plants.

To further test whether CDF4 is a direct transcriptional regulator of *NCED2* and *NCED3*, we used a LUC (luciferase)-based *trans*-activation experiment. We co-expressed *CDF4* with both *NCED2* and *NCED3* promoter-LUC fusion reporters in mesophyll protoplasts of *Arabidopsis*, which resulted in an increase in luciferase activity, although they showed activities only 2.0- and 1.7-fold higher than in the control. To increase transcriptional activity, we used the 35S::*CDF4*-VP16 effector plasmid carrying the VP16 activation domain and observed much greater increases in luciferase activity (Fig 3H and I). Hence, we suggested that *CDF4* probably acted in concert with co-activators that are expressed in mature or senescing rosette leaves. Because young leaves were used for the earlier protoplast isolation in our study, they may not have contained any co-activators. These results implied that CDF4 might bind to the promoters of *NCED2* and *NCED3* to induce their transcription. The (A/T) AAAG/CTTT (T/A) core sequence was reported to be crucial for DOF transcription factor binding. There were 12 and 15 DOF-binding core sequences in the approximately 2.0-kb *NCED2* and *NCED3* promoter sequences, respectively, that were assessed in the trans-activation experiment (Fig 3J).

To provide further evidence for the interaction, chromatin immunoprecipitation (ChIP) assays were conducted to identify whether the CDF4 protein could bind to the gene promoters. pER8::*CDF4*::HA transgenic plants were used, which contained an HA-coding sequence fused in-frame to the 3′ end of the *CDF4* gene. Quantitative real-time ChIP-qPCR assays, using an anti-HA antibody, showed that CDF4 could bind to the conserved sequence motifs in the *NCED2* and *NCED3* gene promoters (Fig 3K). We also performed *in vitro* DNA–protein interaction ELISA (DPI-ELISA) experiments with an epitope-tagged CDF4 protein. A native-sequence oligonucleotide, containing the functional DOF-binding sites derived from the *NCED2* and *NCED3* promoter sequences and the mutated version, was used (Appendix Fig S12A–C). The result shows a positive correlation between the amount of glutathione S-transferase (GST)-CDF4 detected with the epitope-specific antibody, indicating that GST-CDF4 bound to the wild-type oligonucleotide in a concentration-dependent manner. As shown in Appendix Fig S12, the wild-type, but not the mutated, oligonucleotide was able to reduce the amount of GST bound to the plate, thus confirming the specificity of the binding. We further performed the EMSA to verify the binding of *CDF4* to the selected D3 and D4 domains of *NCED2* gene promoter and D5 and D6 domains of *NCED3* gene promoter (Appendix Fig S13A and B). These results demonstrated that CDF4 could target the *NCED2* and *NCED3* gene promoters and induce their transcription.

Mutation of *NCED2* and *NCED3* suppresses ABA accumulation and leaf senescence in pER8::*CDF4*

Our data indicated that CDF4 was involved in the control of leaf senescence by targeting the *NCED2* and *NCED3* promoters. Moreover, we wanted to determine whether the expression of *NCED2* and *NCED3* genes was related to leaf senescence control. To address this question, we measured the expression of *NCED2* and *NCED3* in senescing leaves. As with *CDF4* expression, they exhibited high levels of expression in the leaf tip (Fig 1C). The temporal expression patterns of the *NCED2* and *NCED3* genes were similar to that of *CDF4* (Fig 4A and C). Expression of *NCED2* and *NCED3* was upregulated during the leaf senescence process, but their expression was significantly reduced in the *CDF4::*RNAi plants, implying that *NCED2* and *NCED3* played an important role in CDF4-mediated control of leaf senescence (Fig 4B and D). Interestingly, we also detected an increase in *CDF4* expression in the plants that constitutively overexpressed *NCED2* and *NCED3*, which is consistent with the finding that *CDF4* expression is induced by ABA (Appendix Fig S14A–D).

To determine whether ABA accumulation in *CDF4*-overexpressing plants depends on *NCED2* and *NCED3*, we obtained *NCED2* and

NCED3 T-DNA insertion knockout mutants (Appendix Fig S15A–C). A decrease in *CDF4* transcript levels was observed in these *nced2* and *nced3* mutants (Appendix Fig S15D), which supported the hypothesis that *NCED2/3*-mediated ABA biosynthesis and *CDF4* expression mutually promoted one another. Then, a pER8::*CDF4* transgenic plant was crossed with the *nced2*, *nced3*, and *nced2nced3*

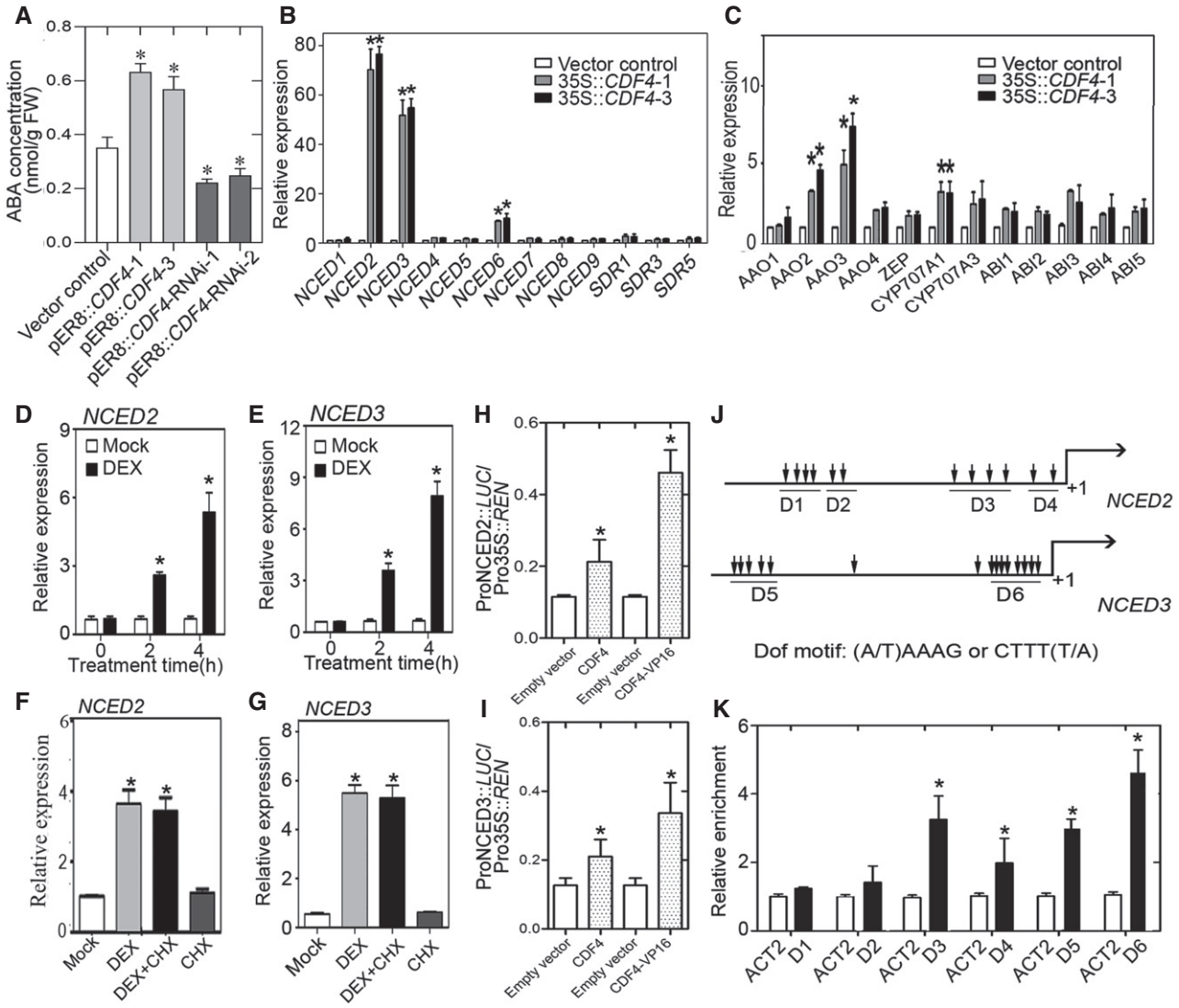

Figure 3. *CDF4* is involved in ABA biosynthesis by directly activating the transcription of *NCED2* and *NCED3*.

A Measurement of free ABA levels in the third and fourth rosette leaves from 21-day-old transgenic lines with altered *CDF4* expression after estradiol induction for 3 days (once every day). Three independent experiments were conducted. Values are given as mean ± SD, $n = 3$. *$P < 0.05$ by Student's *t*-test.

B, C qPCR analysis of ABA synthesis and signaling-related genes in Col-0 and 35S::*CDF4* plants. Three independent experiments were conducted. Values are given as mean ± SD, $n = 3$. *$P < 0.05$ by Student's *t*-test.

D, E Relative expression of *NCED2* and *NCED3* in 14-day-old *CDF4GR* transgenic plants treated with 20 μM β-estradiol or mock treatment for 0, 2, or 4 h. The expression of the corresponding genes in mock-treated plants was set to 1.0. Three independent experiments were conducted. Values are given as mean ± SD, $n = 3$. *$P < 0.05$ by Student's *t*-test.

F, G Relative expression level of *NCED2* and *NCED3* in 14-day-old *CDF4*GR transgenic plants treated with 20 μM DEX, 100 μM CHX, DEX plus 100 μM CHX, or mock. The gene expression in mock-treated plants was set to 1.0. Three independent experiments were conducted. Values are given as mean ± SD, $n = 3$. *$P < 0.05$ by Student's *t*-test.

H Schematic diagram indicating the locations of six DOF motif clusters (D1–D6) in the *NCED2* and *NCED3* gene promoters.

I ChIP-qPCR analysis of the ability of CDF4 to bind to the promoters of *NCED2* and *NCED3*. An anti-HA monoclonal antibody was used for DNA immunoprecipitation from 3-week-old pER8::*CDF4*-HA transgenic plants. Black bars indicate the enrichment fold changes normalized to that of ACT2. Three independent experiments were conducted. Values are given as mean ± SD, $n = 3$. *$P < 0.05$ by Student's *t*-test.

J, K Transient dual-luciferase reporter assay. The pGreenII-0800 LUC construct containing the *CDF4* promoter and the p62-SK construct with or without the *CDF4* coding region and CDF4-VP16 were transiently co-transformed into Col-0 protoplasts. Firefly luciferase (LUC) and Renilla luciferase (REN) activities were measured after culturing the protoplasts under low light conditions for 16 h. The ProNCED2/3:LUC/Pro35S:REN ratio represents the relative activities of *NCED2* and *NCED3* transcription. Three independent experiments were conducted. Values are given as mean ± SD, $n = 3$. *$P < 0.05$ by Student's *t*-test.

double mutants. pER8::*CDF4* & *nced2*, pER8::*CDF4* & *nced3*, and pER8::*CDF4* & *nced2nced3* plants had higher *CDF4* expression after induction with estradiol (Appendix Fig S16). We analyzed the progression of senescence in the vector control line and in various transgenic lines. Under normal growth conditions, pER8::*CDF4* & *nced2* and pER8::*CDF4* & *nced3* rosette leaves exhibited delayed senescence compared with pER8::*CDF4* after induction with estradiol (Fig 4E). In addition, the pER8::*CDF4* & *nced2* and pER8::*CDF4* & *nced3* rosette leaves showed decreased *SAG12* expression (Fig 4F), increased chlorophyll content (Fig 4G), and suppressed *CDF4*-induced leaf senescence compared with the pER8::*CDF4* plants. Moreover, pER8::*CDF4* overexpression in the *nced2nced3* mutant background further delayed the leaf senescence phenotype to the vector control level (Fig 4E–G). We also found that the *nced2nced3* double mutant, rather than the *nced2* and *nced3* single mutants, delayed the aging process of leaves (Appendix Fig S14E). Taken together, we concluded that the loss of *NCED2* and *NCED3* function suppressed ABA production and leaf senescence progression in plants overexpressing *CDF4*.

CDF4-RNAi plants exhibit enhanced tolerance to oxidative stress

The endogenous levels of H_2O_2 gradually increased during the leaf senescence process, and the accumulated H_2O_2 played an important role in the development of characteristics associated with senescence. Based on our findings showing the induction of *CDF4* expression by H_2O_2 (Fig 1F), we next wanted to determine whether *CDF4* participated in the regulation of oxidation-related leaf senescence. We examined the H_2O_2-induced senescence phenotype in the vector control and the transgenic plant leaves under dark conditions. When subjected to H_2O_2 treatment for 3 days, all pER8::*CDF4* detached leaves turned yellow, while detached leaves of the vector control plants were pale green, but the detached *CDF4*-RNAi leaves largely remained fully green (Fig 5A). DAB (3,3′-diaminobenzidine)

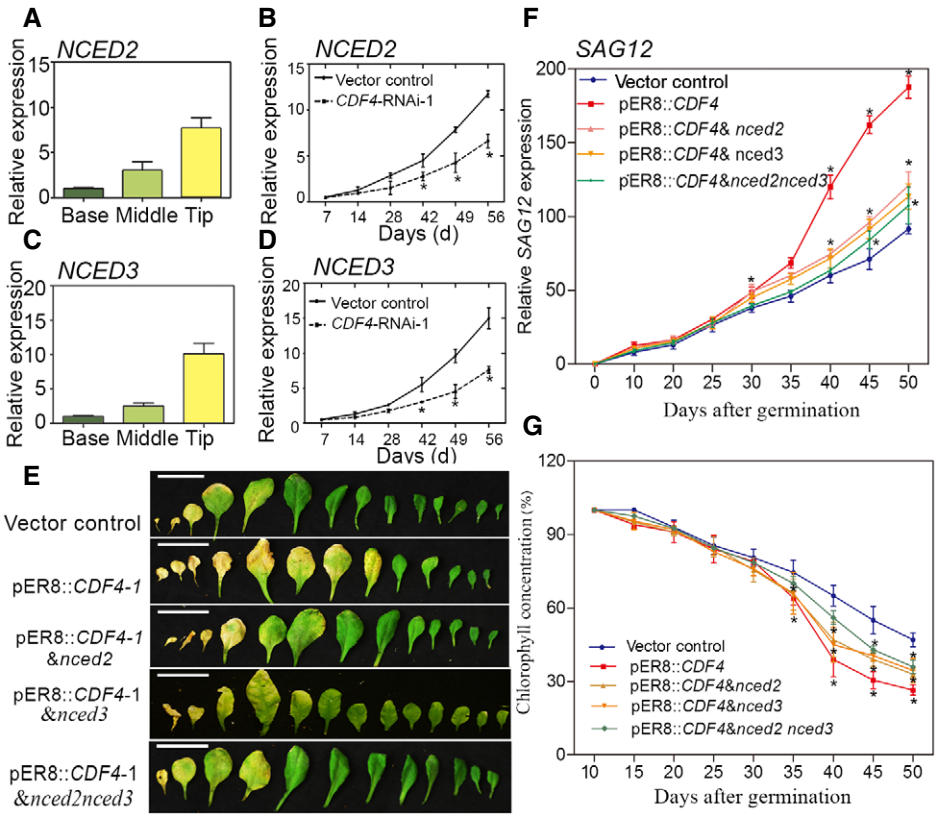

Figure 4. Involvement of *NCED2* and *NCED3* in the progression of leaf senescence in the vector control, pER8::*CDF4*, pER8::*CDF4* & *nced2*, pER8::*CDF4* & *nced3*, and pER8::*CDF4* & *nced2nced3* plants.

A–D Transcript levels were determined by qPCR and normalized to *AtACT2*. (A, C) Localized *NCED2* and *NCED3* expression in the wild-type senescing leaf. Half-senesced leaves were split into three parts, as shown in Fig 1A and C. (B, D) *NCED2* and *NCED3* expression during leaf senescence in the vector control and *CDF4*-RNAi-1 plants. Transgenic plant leaves were analyzed from 7 to 56 d (d, days after planting). Four independent experiments were conducted. Values are given as mean ± SD, $n = 4$. *$P < 0.05$ by Student's *t*-test.

E Observation of rosette leaf longevity from the 26-day-old vector control, pER8::*CDF4*, pER8::*CDF4* & *nced2*, pER8::*CDF4* & *nced3*, and pER8::*CDF4* & *nced2nced3* transgenic plants after 20 μM estradiol induction for 2 weeks. Phenotype of detached rosette leaves arranged from oldest to youngest. Scale bars indicate 1.5 cm.

F, G (F) *SAG12* expression level and (G) chlorophyll concentration in rosette leaves in (E) at various development stages. Three independent experiments were conducted. Values are given as mean ± SD, $n = 4$. *$P < 0.05$ by Student's *t*-test.

Source data are available online for this figure.

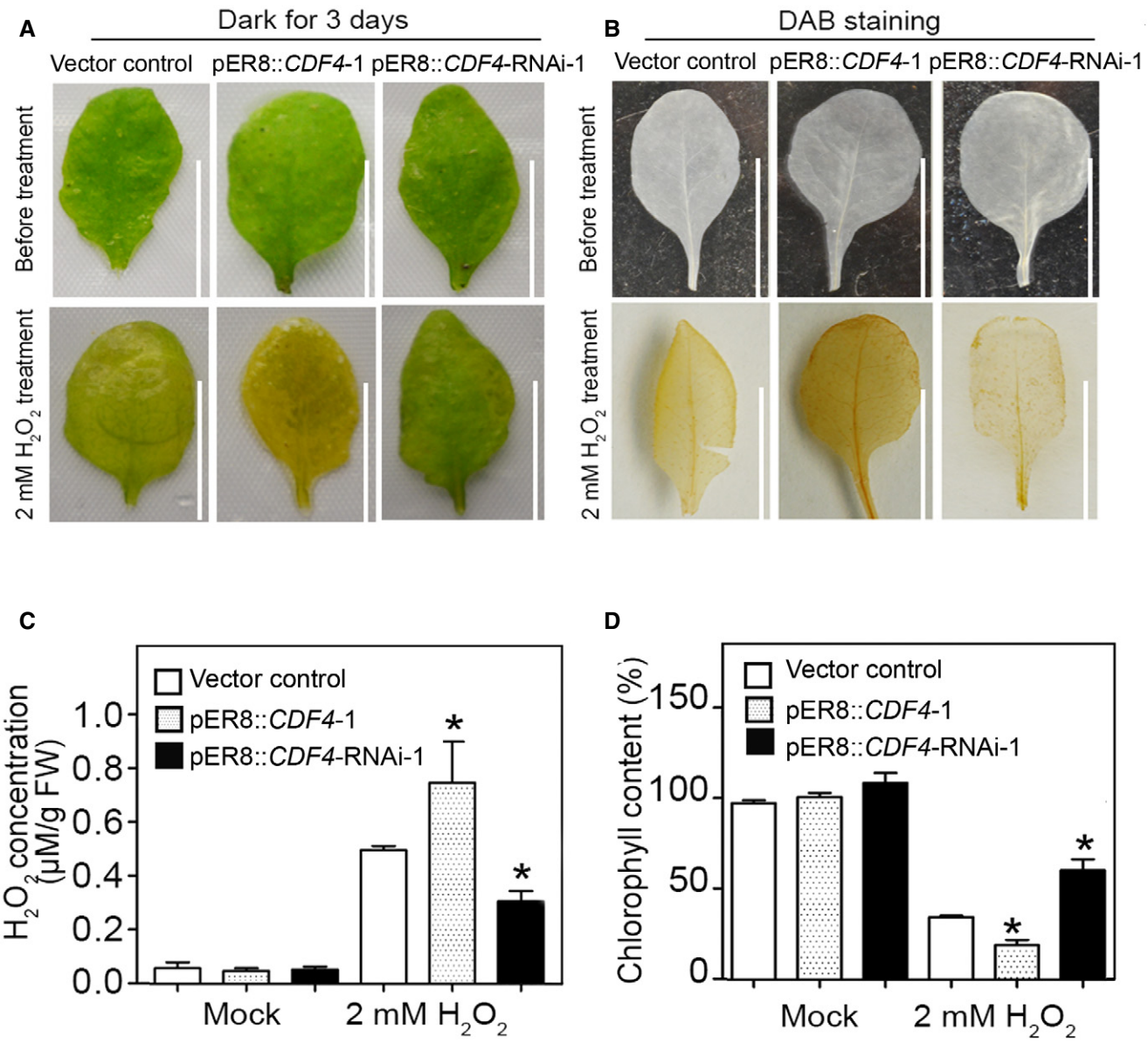

Figure 5. CDF4 suppresses H_2O_2 scavenging.

A The senescence phenotype of the vector control, pER8::CDF4, and pER8::*CDF4*::RNAi detached leaves treated with H_2O_2 and incubated in the dark for 3 days. The third leaf in rosettes of 3-week-old plants was detached and incubated in MES buffer (2 mM MES, pH 5.8) treated with 2 mM H_2O_2 and 20 μM β-estradiol under dark conditions for 3 days. Picture shows the leaves before and after treatment. Scale bars indicate 1 cm.

B, C (B) DAB staining and (C) measurement of H_2O_2 before and after 2 mM H_2O_2 plus 20 μM β-estradiol treatment under dark conditions for 2 days. The brown color represents H_2O_2 accumulation. Three independent experiments were conducted. Values are given as mean ± SD, $n = 3$. *$P < 0.05$ by Student's *t*-test. Scale bars indicate 1 cm.

D Chlorophyll concentrations in the leaves shown in (A). Three independent experiments were conducted. Values are given as mean ± SD, $n = 3$. *$P < 0.05$ by Student's *t*-test.

staining and quantitative measurements of H_2O_2 also revealed that *CDF4*-RNAi leaves accumulated less endogenous H_2O_2 than did either the vector control or the pER8::*CDF4* leaves in response to exogenous H_2O_2 application (Fig 5B and C). Measurement of chlorophyll concentration in dark/H_2O_2-treated vector control and transgenic plant leaves supported the observed phenotype (Fig 5D). The DAB staining showed that, following exogenous H_2O_2 treatment, *CDF4*-RNAi leaves displayed less H_2O_2 accumulation than did the vector control leaves, implying that *CDF4*-RNAi leaves had greater H_2O_2 scavenging capacity (Fig 5B). Furthermore, similar results were obtained from comparisons of vector control and pER8::ami*CDF4* transgenic plants (Fig 2E). Taken together, downregulation of *CDF4* expression enhanced tolerance to oxidative stress and delays leaf senescence.

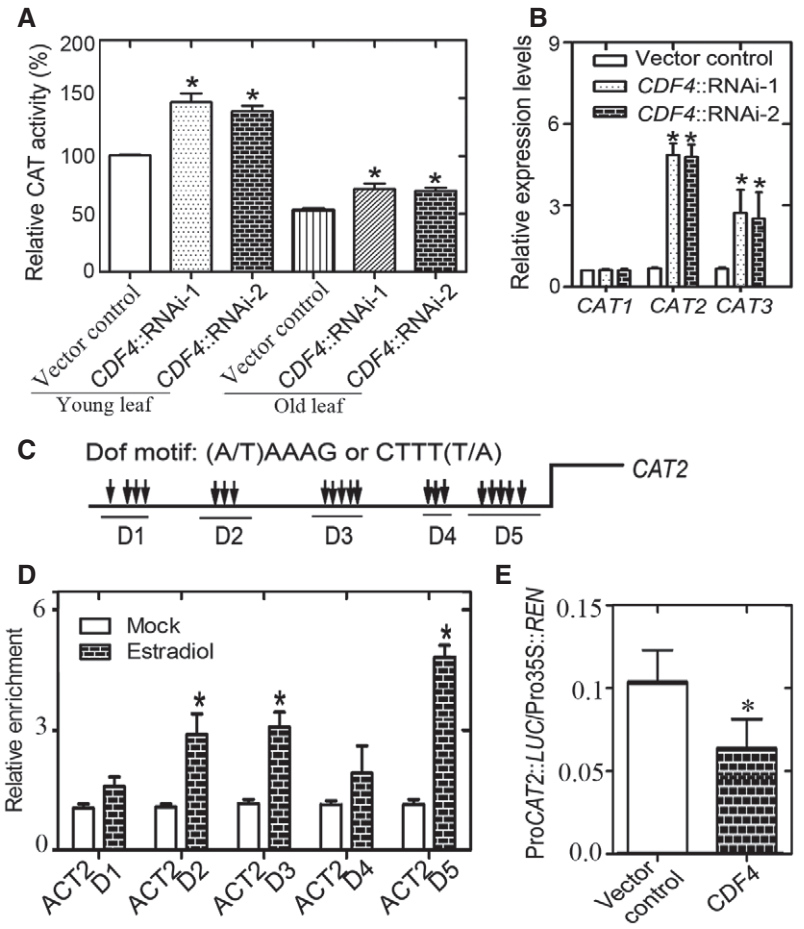

Figure 6. CDF4 suppresses catalase activity by repressing CAT2 transcription.

A Measurement of catalase activity in vector control and CDF4RNAi plants. Ten-day-old green seedlings ("Young") and the third and fourth rosette leaves from 36-day-old plants ("Old") were used, respectively. Three independent experiments were conducted. Data are represented as means ± SD, $n = 3$. Student's *t*-test, $*P < 0.05$.

B qPCR analysis of *CAT* genes expression in the third and fourth rosette leaves from 36-day-old plants. The expression of *CAT* genes in the wild-type plant is given as 1. Three independent experiments were conducted. Data are represented as means ± SD, $n = 3$. Student's *t*-test, $*P < 0.05$.

C Schematic diagram indicating the locations of the putative CDF4-binding motif clusters (D1–D5) in the promoter of *CAT2*.

D ChIP-qPCR analysis of the relative binding of CDF4 to the promoter of *CAT2*. An anti-HA monoclonal antibody was used for DNA immunoprecipitation from 32-day-old pER8::*CDF4*-HA transgenic plants. Black columns indicate the enrichment fold changes normalized to that of ACT2. Three independent experiments were conducted. Data are represented as means ± SD, $n = 3$. Student's *t*-test, $*P < 0.05$.

E Transient dual-luciferase reporter assay. The pGreenII-0800 LUC construct containing the *CAT2* promoter and the p62-SK construct with or without CDF4 were transiently co-transformed into Col-0 protoplasts. Firefly luciferase (LUC) and Renilla luciferase (REN) activity were measured after culturing the protoplasts under low light conditions for 16 h. Six independent experiments were conducted. Values are given as mean ± SD, $n = 6$. $*P < 0.05$ by Student's *t*-test.

CDF4 suppresses catalase (CAT) activity by repressing *CAT2* transcription

Given that *CDF4*-RNAi plants showed reduced H_2O_2 accumulation and enhanced tolerance to exogenous H_2O_2 treatment, we investigated the relationship between *CDF4* expression and the activity of H_2O_2 scavengers. Plants contain several antioxidant enzymes or proteins. Catalases (CATs) are primarily responsible for H_2O_2 scavenging. We first measured CAT activity, and found that *CDF4*-RNAi plants exhibited higher CAT activities in both young and old leaves compared with the vector control (Fig 6A), indicating that *CDF4* suppresses CAT activities. There are three catalase genes in the *Arabidopsis* genome. We found that the expression of *CAT2* and *CAT3*, but not *CAT1*, was induced in *CDF4*-RNAi plants (Fig 6B). Because *CAT2* is the major catalase isoform and expression of only *CAT2* declined in 35S::*CDF4* transgenic plants (Appendix Fig S17A), we focused our analysis on *CAT2*. Interestingly, many DOF-binding motif clusters were found in the promoter of the *CAT2* gene (Fig 6C). Furthermore, we tested whether *CDF4* could directly regulate *CAT2* at the transcriptional level. ChIP assays were conducted using pER8::*CDF4*::HA transgenic plants to identify whether the CDF4 protein binds to the *CAT2* promoter. ChIP-qPCR assays, using an anti-HA antibody, indicated that CDF4 could bind to the selected regions in the *CAT2* promoter (Fig 6D). In addition, dual-LUC reporter assays revealed that CDF4 repressed *CAT2* transcription in *Arabidopsis* protoplasts (Fig 6E). *In vitro* DPI-ELISA experiments, performed with an epitope-tagged CDF4 protein, also verified that CDF4 binds selected DOF-binding motif clusters in the *CAT2*

promoter (Appendix Fig S12D). We further performed the EMSA to verify the binding of *CDF4* to the D2, D3 and D5 domains of *CAT2* gene promoter (Appendix Fig S13C). All together, these results demonstrated that *CDF4* repressed catalase activity by inhibiting *CAT2* transcription.

Moreover, we also determined the expression of other genes encoding H_2O_2-scavenging enzymes, such as ascorbate peroxidases (APXs) and superoxide dismutases (SODs). Eight ascorbate peroxidase genes have been annotated on the *Arabidopsis* genome. We found that the expression of *APX4-6*, *sAPX*, and *tAPX*, but not *APX1-3*, was changed in the *CDF4* transgenic plants (Appendix Fig S17B and C). Among them, *APX5* expression was obviously affected in *CDF4* transgenic plants (Appendix Fig S17B and C). In addition, the lower abundance levels of several SOD transcripts in 35S::*CDF4* leaves indicated that *CDF4* also repressed their expression (Appendix Fig S17D).

Increased CAT activity suppresses the early-senescence phenotype of *CDF4* overexpression

Given our findings that *CDF4* suppressed *CAT2* transcription, we investigated whether the increase in catalase activity in pro*SAG12*::*CDF4* plants could suppress their early-leaf-senescence phenotype. To address this question, we generated pro*SAG12*::*CDF4* & 35S::*CAT2* transgenic plants by crossing pro*SAG12*::*CDF4* into the 35S constitutive *CAT2*-overexpressing plant background. We found that the *CAT2* gene overexpression partly rescued the early-senescence phenotype of pro*SAG12*::*CDF4*, with a reduced number of yellow leaves (Fig 7A), and *CDF4* gene expression levels were high in the transgenic plants (Fig 7B). Consistent with the visible phenotype, the increase in H_2O_2 level and reduction in chlorophyll concentration observed in pro*SAG12*::*CDF4* plants were suppressed by *CAT2* gene overexpression (Fig 7C–E). Interestingly, consistent with previous results, the *cat2* knockout mutant showed an early-senescence phenotype (Appendix Figs S15A, E, F and S18A). However, 35S::*CAT2* plants in the Col-0 background displayed a leaf senescence phenotype similar to that of Col-0, implying that the H_2O_2-scavenging activities are probably controlled at an adequate level during normal development (Appendix Fig S18B and C). These results suggested that the elevated H_2O_2 concentration in pro*SAG12*::*CDF4* plants served as another mechanism underlying their accelerated leaf senescence phenotype.

CDF4 promotes floral organ abscission in *Arabidopsis*

Senescence usually occurs synchronously with the abscission process in *Arabidopsis*. For example, in the abscission-delayed *etr1-1* mutant, the leaf senescence process is slowed [66]. Here, we found a similar situation. Our study shows that *CDF4* may play a role in the floral organ abscission regulation, because *CDF4* was specifically expressed in the floral organ abscission zone (Appendix Fig S3B and C) and the clearly altered abscission process was observed in the plants overexpressing or downregulating expression of the *CDF4* gene under the control of the floral organ abscission-related peptide ligand INFLORESCENCE DEFICIENT IN ABSCISSION (*AtIDA*) promoter (Fig 8A and Appendix Fig S21). Given that CDF4 belongs to the DOF transcription factor family, we were interested in determining whether it regulates the expression of genes involved in abscission. Several components, with putative functional enzymatic activities or signaling roles in abscission, were selected for analysis of their expression levels. Combining transcriptome data with our qPCR analysis, the transcript levels for most of the selected genes, namely *ADGP1*, *PGAZAT/ADPG2*, *QTR2*, *AtDOF4.7*, *HWS*, *HAESA*, *IDA*, *AGL15*, *AtEXP10*, *ARP4,* and AT3G14380, were checked in positions 5–6 of young siliques of the control and the *CDF4*-overexpression lines (Fig 8B). There were no significant changes in expression, except for the three polygalacturonase (PG) genes, *ADGP1*, *PGAZAT*, and *QTR2*. The level of expression of *PGAZAT* gene showed the greatest change. ADPG1, PGAZAT, and QUARTET2 are polygalacturonases required for cell separation during reproductive development in *Arabidopsis* [67]. The relative *PGAZAT* expression ratios between the overexpression lines and the wild type were 28 in line 1 and 26 in line 3, with the *PGAZAT* gene expression level being obviously inhibited in the *CDF4* knockdown lines (Fig 8C). These results showed that *PGAZAT* gene expression was obviously upregulated by *CDF4* overexpression. In addition, when proIDA::*CDF4* was crossed with the proPGAZAT::GUS line, the proIDA::*CDF4* & proPGZAT::GUS plants significantly enhanced GUS staining activity compared with the proPGAZAT::GUS plants (Fig 8E). We also found that pER8:*CDF4* and pER8:*CDF4*-RNAi showed the altered floral abscission phenotype after a period of estradiol induction (Appendix Fig S19).

Furthermore, to examine whether the CDF4 protein regulates *PGAZAT* expression by binding to the promoter region, five regions with many DOF protein-binding *cis*-acting elements were selected for analysis (Fig 8D) [47]. For ChIP analysis, formaldehyde cross-linked chromatin from transgenic plants was fragmented and immunoprecipitated with the HA antibody. The PCR product of the *PGAZAT* promoter was enriched in pER8::*CDF4*-HA (Fig 8F). We further performed the EMSA to verify the binding of *CDF4* to the D4 and D5 domains of *PGAZAT* gene promoter (Appendix Fig S13D). The conclusion was that CDF4 targeted the *PGAZAT* gene and induced its expression. The expression of some endoglucanases, that are related to abscission, is also regulated by abscission signals, such as ABA and hydrogen peroxide [67,68]. Further investigation of the role of the two in promoting floral organ abscission is to be studied in the next step of our research. Taken together, our results from the *CDF4* gene studies provide novel insights into the regulation of the activation of the abscission enzymes. These results showed that the CDF4 transcription factor integrated both ABA biosynthesis and endogenous H_2O_2 concentration to modulate leaf longevity and floral organ abscission. Overall, a proposed feedback loop model, involving *CDF4*, ABA and ROS, is shown in Fig 9.

Discussion

Plant senescence is a well-controlled developmental process that is largely regulated genetically. It ultimately leads to cell disintegration. Senescence clearly cannot occur in young leaves. It is possible that senescence-associated inhibitors block the senescence program when leaves are young, while senescence-related activators are turned on as the leaf ages. From molecular and genetic perspectives, many methods have been used to identify genes with changes in expression during leaf senescence. In such a genetic pathway, the activated transcription factors will turn on expression of a large

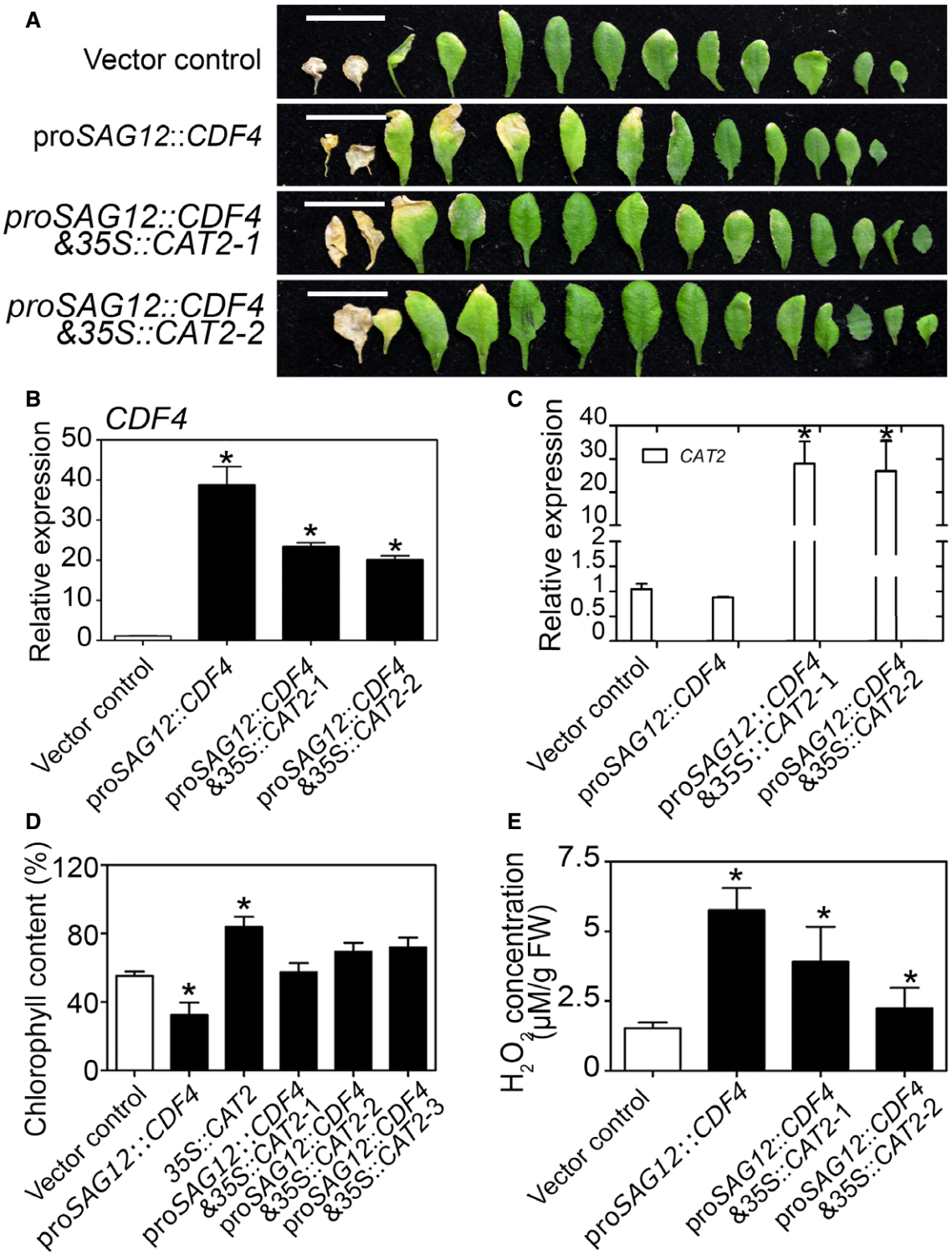

Figure 7. Overexpression of *CAT2* represses proSAG12::*CDF4* early-senescence phenotype.

A The senescence phenotypes of 5-week-old vector control, proSAG12::*CDF4*, and proSAG12::*CDF4* & 35S::*CAT2* plants, from old to young. Scale bars indicate 1.5 cm.

B qPCR analysis of the expression of *CDF4* and *CAT2* in the leaves shown in (A). Four independent experiments were conducted. Values are given as mean ± SD, $n = 4$. *$P < 0.05$ by Student's *t*-test.

C qPCR analysis of the expression of *CAT2* in the leaves shown in (A). Four independent experiments were conducted. Values are given as mean ± SD, $n = 4$. *$P < 0.05$ by Student's *t*-test.

D, E (D) Measurement of chlorophyll and (E) H_2O_2 concentrations in the leaves shown in (A). The third leaves in the rosette were used. Four independent experiments were conducted. Data are presented as the mean ± SD, $n = 4$. *$P < 0.05$ by Student's *t*-test.

number of leaf senescence-related genes. Thus, the isolation and molecular characterization of leaf senescence-related transcription factors will aid in understanding their roles in regulating gene expression. CDF4 belongs to the subfamily A or type II DOF family proteins [47,59]. CDF4 had previously been identified as a nucleus-localized transcription factor; WOX5 represses CDF4 transcription by recruiting TPL/TPR and HDA19 at the CDF4 regulatory region. CDF4 promotes columella cell differentiation, and its repression by WOX5 is essential to maintain CSCs in an undifferentiated state [63]. However, the mechanism of CDF4 involvement in leaf senescence regulation was unknown. Here, the *CDF4* gene was isolated as a new leaf senescence-related transcription factor gene. Expression analyses revealed that the *CDF4* mRNA level increased at the late stage of leaf senescence (Fig 1C and D). This profile indicated that senescence could be controlled via the transcriptional regulation of genes involved in leaf senescence. To verify the function of *CDF4*, leaf senescence phenotypes in *CDF4* transgenic lines were investigated. The leaf phenotype observed in 35S::*CDF4* mainly proceeded via a senescence-related pathway because the reliable senescence marker *SAG12* was easily detected in these transgenic lines (Fig 2B). In addition, we observed inhibited cell expansion in 35S::*CDF4* plants as a result of downregulation of cell elongation factors. Interestingly, the ability to inhibit cell expansion has been observed in many DOF family genes, implying that this function is conserved during evolution [48,50,51,53–55]. However, the phenotype of premature senescence in the rosette leaves was not found in other DOF transgenic plants, indicating that the promotion of plant dwarfing by overexpression of DOF family genes was not the direct cause of early leaf senescence. Our data supported the conclusion that *CDF4* played an important role in the control of leaf senescence. The first evidence was derived from plants in which the constitutive and inducible overexpression of *CDF4* promoted early leaf senescence (Fig 2A and B). Additional evidence was obtained from assays in which *CDF4* was downregulated by RNAi- and amiRNA-mediated gene silencing; these transgenic lines exhibited delayed developmental and H_2O_2-inducible leaf senescence (Fig 2C and D).

Leaves start from leaf primordia and develop into photosynthetic organs through vegetative growth and maturation, which is completed through the coordination of cell division, expansion, and differentiation, and finally enter the senescence stage [1]. Previous study on components of cytokinin and auxin signaling has demonstrated the relevance between leaf growth and senescence. For example, triple mutations of *Arabidopsis* HISTIDINE KINASE 2 (AHK2), AHK3, and AHK4 result in a smaller leaf size, as a result of reduced cell proliferation and early leaf senescence [69]. Cytokinin response factors (CRFs) have been implicated in the control of leaf growth and senescence in *Arabidopsis* [70]. In addition, the AUXIN RESPONSE FACTOR 2 (ARF2) mutation enhances leaf growth and retards leaf senescence [71]. Our knowledge of the interrelationship between early leaf development and senescence is still limited. Here, we identified that *CDF4* mediates cell expansion and senescence during leaf development. As mentioned here, in addition to the positive leaf senescence regulator *CDF4*, *JUB1* is another TF related to leaf senescence. Both of them have the same effect of inhibiting cell extension and regulating the aging phenotype of leaves. However, the difference is that *CDF4* suppresses H_2O_2 scavenging production by inhibiting the expression of *CAT2*, meanwhile promoting the aging process of leaves by upregulating endogenous ABA levels. But *JUB1* overexpression strongly delays senescence, dampens intracellular H_2O_2 levels, and enhances stress tolerance and the induction of *DREB2A* expression. The growth of plants is accompanied by the increase of cell volume and the change of cell wall rigidity and the cell wall collapses during the late senescence phase of leaf development. Therefore, the regulation of cell wall plasticity and cell size is closely related to leaf senescence process. Thus, we believe that *CDF4* might provide us with a good opportunity of investigating the mechanisms involved in mediating leaf development and senescence. This result also implies the relationship between plant regulation of leaf senescence and cell size regulation.

Leaf senescence occurs slowly and is associated with the efficient transfer of nutrients from the senescing leaves to the developing parts of the plant. Promotion of leaf senescence by ABA is a long-term response that allows survival under extreme conditions. The DOF domain protein family is involved in various plant-specific physiological processes. By selecting a probable senescence-related DOF transcription factor, our assay revealed that CDF4 promotes leaf senescence, in part, through upregulated ABA biosynthesis. Because the *CDF4* mRNA abundance was increased when leaf senescence was accelerated by the senescence-accelerating hormone ABA, we also found that dark-induced senescence in detached leaves was accelerated in *CDF4*-overexpressing plants (Fig 2E). Further studies have indicated that CDF4 regulates leaf senescence by increasing ABA biosynthesis as a result of targeting the key ABA biosynthesis genes, *NCED2* and *NCED3*. The *nced2* and *nced3* knockout mutants delayed *CDF4*-induced leaf senescence (Fig 4E). In order to provide a more in-depth insight into the role of *CDF4* for ABA-mediated regulation of leaf senescence, we measured the stomatal aperture of vector control and *CDF4* transgenic plants. The results showed that stomatal aperture obviously decreased in *CDF4* overexpression plant leaves and increased in *CDF4* knockdown plants (Appendix Fig S20). The change of stomatal aperture may be due to the effect of *CDF4* regulating ABA content in plants. These results indicated that the change of stomatal aperture was involved in *CDF4*-induced leaf senescence. Taken together, we conclude that the CDF4 protein plays a role in integrating developmental age and environmental stimuli to initiate the leaf senescence process. A recent report has indicated that the mitochondrial protease FtSH4 promotes leaf senescence by inducing the expression of WRKY transcription factor genes as well as promoting ABA accumulation [72]. Furthermore, the *wrky70wrky54* double mutant exhibits increased ABA levels and exhibited an early-senescence phenotype [73]. These results have verified the important role of ABA in controlling leaf senescence.

In addition to promoting ABA biosynthesis, we discovered that *CDF4* also functions in plant tolerance to oxidative signals such as H_2O_2. Exogenous application of H_2O_2 can dramatically accelerate the leaf senescence process, particularly in the dark. Downregulation of *CDF4* led to enhanced tolerance to the effects of exogenous H_2O_2 application, as less endogenous H_2O_2 accumulated and higher chlorophyll concentration occurred in rosette leaves (Fig 5A–D). One of the reasons behind this effect was the increased catalase activity in *CDF4* RNAi plants, which was due mainly due to the upregulation of expression of *CAT2*. Like *NCED2* and *NCED3*, *CAT2* is a target gene of *CDF4*, although the regulatory mechanisms of these two classes of gene were different. We identified various DOF-

binding motifs in the promoter of *NCED2* and *NCED3* that mediated their induction by *CDF4*, whereas the DOF-binding motifs in the promoter of *CAT2* mediated their repression by *CDF4*. Currently, it is not known how these seemingly identical DOF-binding sequences play opposite roles in mediating *CDF4*-directed effects on transcription. Exogenous application of H_2O_2 can dramatically accelerate the

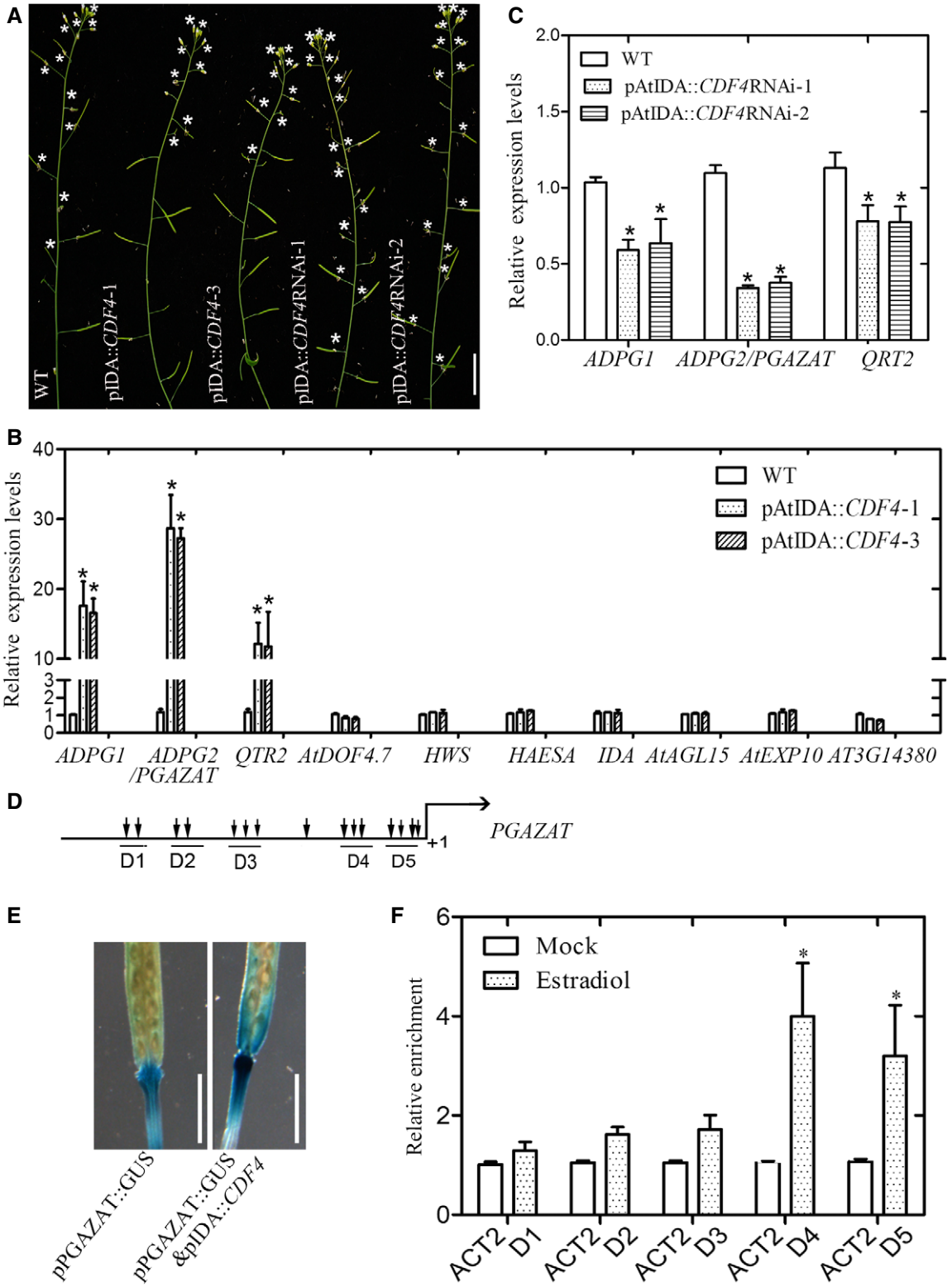

Figure 8.

Figure 8. Altered floral organ abscission process in the *CDF4* transgenic plants.

A–C (A) Observation of inflorescences of 7-week-old wild-type (WT) *Arabidopsis* and the *CDF4* transgenic plants. The asterisk represents the flower organ attached along the inflorescence. Scale bar indicates 1.5 cm. Selected abscission-related gene expression levels in (B) WT and proIDA::*CDF4* lines or (C) WT and proIDA::*CDF4*RNAi lines by using qPCR analysis. The expression of these selected genes in the wild-type plant is given as 1. The relative expression level represents only the level of expression of the gene relative to the wild type. *ACTIN2* was used as the internal control. Three independent experiments were conducted. Values are given as mean ± SD, $n = 3$. *$P < 0.05$ by Student's *t*-test.

D Schematic diagram indicating the locations of the putative CDF4-binding motif clusters (D1–D5) in the approximately 1.8-kb promoter of *PGAZAT*.

E Observation of GUS staining activity in the proPGAZAT::GUS and proPGAZAT::GUS & proIDA::*CDF4*. Scale bar indicates 0.5 cm.

F ChIP-qPCR analysis of the relative binding of CDF4 to the promoter regions of *PGAZAT*. An anti-HA monoclonal antibody was used for DNA immunoprecipitation from 6-week-old pER8::*CDF4*-HA transgenic plants after estradiol induction. Black columns indicate the enrichment fold changes normalized to ACT2. Three independent experiments were conducted. Values are given as mean ± SD, $n = 3$. *$P < 0.05$ by Student's *t*-test.

leaf senescence process. Knockdown of *CDF4* led to enhanced tolerance to exogenous H_2O_2 application, as less endogenous H_2O_2 accumulated in plant rosette leaves (Fig 5C). Given that the downstream regulatory networks dictated by *CDF4* in these processes are still unclear, our findings about the regulatory role of *CDF4* in ABA biosynthesis and ROS scavenging in leaf senescence offer a potential mechanism for these developmental processes as well. It is conceivable that, upon leaf senescence, age-dependent *CDF4* expression progressively leads to concomitant increases in ABA and H_2O_2 levels, two well-defined inducers of leaf senescence. We also found that *CDF4* expression was induced by ABA and H_2O_2 treatment. Interestingly, ABA and ROS levels are highly correlated, and these compounds mutually induce each other's accumulation in many biological processes [74–78].

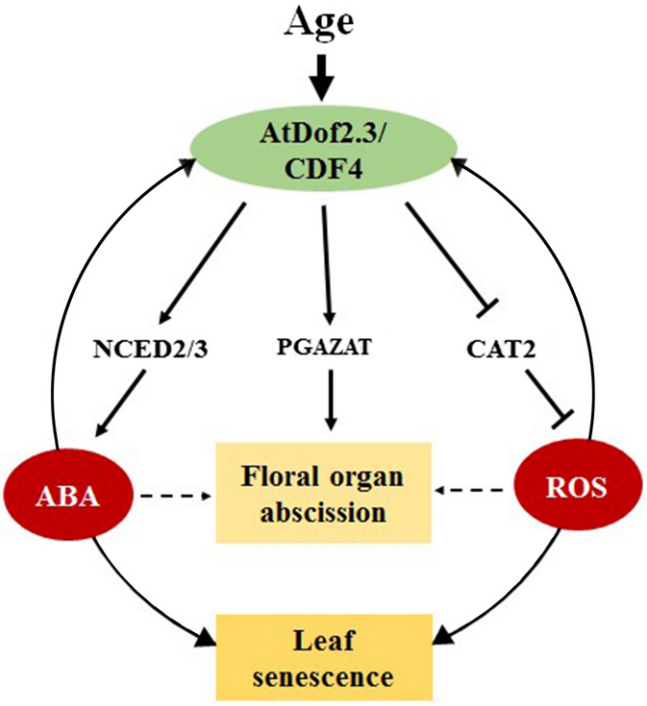

Figure 9. The proposed model illustrating the amplification loop involving *CDF4*, ABA, and ROS.

CDF4 is a senescence-associated gene with expression induced by ABA and ROS, two well-known leaf senescence inducers. CDF4 further promotes ABA biosynthesis by activating the transcription of *NCED2* and *NCED3* and repressing H_2O_2 scavenging by inhibiting *CAT2* transcription. At the same time, *CDF4* can bind to the *PGAZAT* promoter region, thus promoting the floral organ abscission process. Given that ABA and ROS also mutually promote each other's accumulation, *CDF4*, ABA, and ROS form a tripartite amplification loop to accelerate leaf senescence and floral organ abscission. As a result, the levels of CDF4, ABA, and ROS undergo a gradual increase driven by their interlinking positive feedback loops during the leaf senescence and floral organ abscission process. In the legend, the solid and dotted lines represent the direct interaction obtained in this research and indirect interaction, respectively. And the arrow- and T-ending lines represent positive and negative regulatory pathways, respectively.

Floral organ abscission has been used as a model system for studying genetic regulation of the leaf abscission process in *Arabidopsis* [79]. However, little is known about the molecular mechanisms behind signal transduction and cell wall dissolution in abscission. Here, by studying the position of floral organ withering in the wild-type and the *CDF4* transgenic plants, we found that *CDF4* promoted not only leaf senescence but also floral organ abscission. Combining the expression pattern, transcriptome data and quantitative PCR results, we infer that *CDF4* plays important roles in the transcriptional regulation of floral organ abscission. Furthermore, the *in vivo* ChIP experiment confirmed that the effect is mainly realized by regulating the cell wall hydrolase gene, *PGAZAT*. Because *CDF4* can promote the synthesis of ABA and ROS accumulation, and ABA and ROS are two well-known abscission inducing factors, it is possible to propose that, with the increase in leaf age, the increase in *CDF4* gene expression promotes endogenous ABA synthesis and ROS accumulation, thus promoting the floral organ abscission process.

Based on the current findings and previous results, we propose a positive feedback loop model, showing how *CDF4*, ABA, and ROS are responsible for promoting leaf senescence and floral organ abscission (Fig 9). In this model, each of these three players promotes the accumulation of the other two via independent mechanisms. Thus, the levels of CDF4, ABA, and ROS undergo a gradual increase driven by their interlinking positive feedback loops, along with the leaf senescence process. It is straightforward to imagine that suppression of one of them would lead to a slowdown of senescence progression. Although our study established a signaling network involving *CDF4*, ABA, and ROS, other components could also be associated with this loop. Another positive regulator of the amplification loop might be the bZIP transcription factor GBF1, which induces H_2O_2 accumulation by downregulating *CAT2* expression during leaf senescence [80]. A recent report indicated that the WRKY family transcription factor WRKY75 promoted SA accumulation and H_2O_2 accumulation, with WRKY75, SA, and ROS forming an amplification loop to promote the progression of leaf senescence [81]. Taken together, we have found that our positive feedback loop model provides a molecular framework connecting upstream

signals, such as developmental age, ABA, and other environmental stresses, with the downstream regulatory network during leaf senescence and floral organ abscission progression.

Materials and Methods

Plant materials and growth conditions

The Col-0 *A. thaliana* ecotype was used. Plants were grown in a climate-controlled growth room at 22°C (± 2°C) with a relative humidity of 60% under 16-h/8-h light/dark lighting conditions and 120 mmol photons/m^2/s of white light illumination. The *nced2* (SALK_004231), *nced3* (CS331021), *cat2-1* (SALK _057998), and *cat2-2* (SALK_097354) mutants were obtained from the ABRC T-DNA mutant repository. The mutants CS91480 and CS87649 were obtained from the NASC mutant repository. The pER8::*CDF4* transgenic plant was crossed with the *nced2*, *nced3* mutants, and 35S::*CAT2* lines to obtain pER8::*CDF4* & *nced2*, pER8::*CDF4* & *nced3*, pER8::*CDF4* & *nced2nced3,* and pro*SAG12*::*CDF4* & 35S::*CAT2* transgenic plants. T2 transgenic plants were used in our assays. Sequence data for the genes described in this article can be found in the *Arabidopsis* TAIR database (https://www.arabidopsis.org) under the following accession numbers: At2g34140 for *CDF4*, At1g29160 for *COG1*, At4g18350 for *NCED2*, At3g14440 for *NCED3*, At2g14610 for *PR1*, At1g75040 for *PR5*, At3g20770 for *SAG12*, At1g20630 for *CAT1*, At1g58030 for *CAT2*, At1g20620 for *CAT3*, At1g07890 for *APX1*, At3g09640 for *APX2*, At4g35000 for *APX3*, At4g09010 for *APX4*, At4g35970 for *APX5*, At4g32320 for *APX6*, AT4G38000 for *AtDOF4.7*, At3g57510 for *ADPG1*, At2g41850 for *PGAZAT/ADPG2*, At3g07970 for *QRT2,* and At3g18780 for *ACTIN2*. Germplasm used included *nced2* (SALK_004231), *nced3* (GABI_129B08), *cat2-1* (SALK_057998), and *cat2-2* (SALK_097354) mutants.

Construction of plasmids and generation of transgenic plants

To generate transgenic plants overexpressing *CDF4*, *NCED2*, *NCED3,* and *CAT2* genes, cDNAs were subcloned into a CaMV 35S-controlled pHB vector. For inducible *CDF4* overexpression, the *CDF4* open reading frame (ORF) was cloned into the binary vector pER8. For the inducible knockdown of *CDF4*, the approximately 300-bp target sequence was cloned from the genome. This sequence was introduced into the pCAMBIA1301 vector in the sense and antisense orientation. Next, the entire fragment was removed by digesting the pCAMBIA1301-based construct, and the fragment was inserted into pER8 and pHB vectors to produce pER8::*CDF4*-RNAi and pHB::*CDF4*-RNAi. We obtained eleven inducible *CDF4* knockdown transgenic lines, and the highly downregulated lines pER8::*CDF4*::RNAi-1 and pER8::*CDF4*::RNAi-2 were used for our experiments (Appendix Fig S7). For the proSAG12::*CDF4* and proIDA::*CDF4* constructs, the *CDF4* coding sequence (CDS) was fused with the *SAG12* and *IDA* gene promoters, and then assembled into the pCAMBIA1300 vector. For the proIDA::*CDF4*-RNAi construct, the target sequence was introduced into the pCAMBIA1300 vector in the sense and antisense orientation under the control of the *IDA* gene promoter. For artificial microRNA (amiRNA)-mediated gene silencing of *CDF4*, we used the WMD3 online tool (http://wmd3.weigelworld.org/cgi-bin/webapp.cgi) to achieve the design of an amiRNA specific to the *CDF4* coding region, with the artificial miRNA vector pRS300 being obtained from the Weigel Lab. The final fragment was inserted into pHB vector to produce pER8::ami*CDF4* by using *Spe*I and *Xho*I restriction sites. The highly *CDF4* downregulated lines pER8::ami*CDF4*-1 and pER8::ami*CDF4*-2 were used for our experiments (Appendix Fig S7). To generate 4Enhp *CDF4*-*CDF4*GR, the CaMV 35S enhancer tetrad was amplified using pSKI015 as the template and cloned into pQDL4R1 to generate pQDL4R1-4Enh. The GR domain was cloned from pTA7002, and the coding region of *CDF4* was cloned from the cDNA. Both fragments were fused together and cloned into pQDR2L3 vector to generate pQDR2L3-*CDF4*GR. The floral-dip method was used to transform *Arabidopsis*. The primers used for vector construction are shown in Appendix Table S1.

qPCR analysis

Total RNA was isolated using the RNeasy Plant Mini Kit (Qiagen, USA) and stored at −80°C. The RNA samples were treated with DNase to eliminate genomic DNA. Then, 1 mg of total RNA was used for cDNA synthesis using the Novo Script® 1st Strand cDNA Synthesis SuperMix E041 (Novoprotein, China). qRT–PCRs were set up using Hieff® qPCR SYBR Green Master Mix (Yeasen, China). The data were analyzed with LightCycler 96 analysis software 1.1 ($\Delta\Delta C_T$ method). The *AtACT2* gene was used as an internal control. The qRT–PCR primers are shown in Appendix Table S2. All assays were performed in triplicate.

Subcellular localization study

The green fluorescent protein (GFP) signal was observed in the roots of 6-day-old transgenic *Arabidopsis* seedlings, which were constitutively transformed with the35S::GFP::CDF4 construct and analyzed by confocal microscopy (Zeiss LSM510; Jena, Germany).

Estradiol induction assay

The inducible overexpression or inhibition of *CDF4* was induced by spraying whole plants with 20 μM estradiol at specific stages.

DEX induction assay

The rosette leaves of *CDF4*GR transgenic plants were treated with 20 μM DEX in DMSO, 20 μM DEX plus 100 μM CHX, or DMSO (mock). Leaves were collected at the indicated time and placed into liquid nitrogen immediately.

Hormone and abiotic stress treatments

For the dark treatment, leaves were detached and floated on 3 mM 2-(N-morpholino)ethanesulfonic acid (MES) buffer at pH 5.8 for a specific number of days. For the hormone treatment, mature rosette leaves were transferred to Murashige and Skoog (MS) liquid cultures containing 1 μM ABA, 1 mM SA, or 10 μM JA growth hormones. For ETH treatment, 10 μM 1-aminocyclopropane-1-carboxylic acid (ACC) was used. To determine the effects of drought, salinity, or H_2O_2 on gene expression, leaves were transferred to dry 3 M paper or to a liquid culture containing 100 mM NaCl or 2 mM H_2O_2 for a period of time.

Natural and H_2O_2-induced leaf senescence assays

Natural leaf senescence analysis was performed as described previously [82]. The third and fourth rosette leaves of plants at different development stages were used for measurement of the *SAG12* expression level and chlorophyll concentration. For H_2O_2-induced leaf senescence, the third and fourth rosette leaves were detached and incubated in 2 mM EMS buffer (pH 5.8) with 2 mM H_2O_2 under darkness for a period of time.

Measurements of chlorophyll concentration

Chlorophyll was extracted from rosette leaves with N,N-dimethyl formamide and measured as described previously [35].

Stomatal aperture assay

The assay was conducted as previously described with slight modifications [83]. Epidermal peels from plant leaves were incubated for 4 h in a solution containing 10 mM KCl, 0.2 mM $CaCl_2$, and 10 mM MES·KOH (pH 6.15) under white light (300 μmol/m^2/s). The peeled strips were subsequently incubated in a solution containing the same buffer. Guard cells were photographed by using a light microscope equipped with a digital camera. More than 50 stomata apertures were measured for each mutant and WT plant.

Determination of endogenous ABA concentration

Leaves were collected and immediately frozen in liquid nitrogen. Frozen leaves were pulverized, and ABA was extracted as described previously [15]. Quantitative determination of endogenous ABA was performed by the competitive ELISA method using a Phytodetek ABA test kit (Agdia).

DAB staining and H_2O_2 measurements

For DAB staining, tissues were washed three times with phosphate-buffered saline (PBS) buffer, incubated in DAB staining solution (1 mg/mL DAB, 10 mM Na_2HPO_4, and 0.05% Tween 20, pH 3.8) in the dark for 4–8 h, and then decolorized in 95% ethanol. The intensity of brown coloration reflects the H_2O_2 content. Quantitative H_2O_2 measurements were performed using an Amplex Red Hydrogen Peroxide/Peroxidase Assay Kit (Molecular Probes). Briefly, the samples were frozen in liquid nitrogen and ground into a fine powder, and 30 mg of each sample was fully suspended in 200 μl of H_2O_2 extraction buffer (25 mM sodium phosphate buffer, pH 6.5). The extract was centrifuged at 13,500 *g* for 15 min at 4°C, and the supernatant was prepared for the quantitative assay. The absorbance at 560 nm was measured with a TeCAN Infinite F200/M200 (TECAN) spectrophotometer. The H_2O_2 concentrations are reported in μM/g FW.

Protoplast transfection assays

For transient expression assays, several reporter and effector plasmids were constructed. The reporter plasmid contained the firefly luciferase (LUC) gene, which was controlled by a 35S promoter. *CDF4* sequences were fused to the GAL4 DNA-binding domain (BD) coding sequence and cloned into the effector plasmid. Expression of the fusion genes was driven by the 35S promoter. The vector containing the BD sequence represented the negative control. The reporter and effector plasmids were co-transformed into *Arabidopsis* protoplasts. The luciferase assay was performed using the Luciferase Assay System Kit (Promega, Madison, WI, USA).

Transient dual-luciferase reporter system

The approximately 1.8-kb promoter sequences from *NCED2* and *NCED3* and approximately 1.6-kb promoter sequence from *CAT2* were amplified and inserted into the reporter plasmid pGreen II 0800-LUC. The coding sequence of *CDF4* was amplified by PCR and inserted into the effector plasmid pGreen II 62-SK. *Arabidopsis* protoplasts were prepared as described previously [63] and co-transfected with the constructs according to the manufacturer's instructions for the Dual-Luciferase Reporter Assay System (Promega). The ratio of LUC to REN (Renilla luciferase) was determined for the Dual-Luciferase Reporter Assay System (Promega, Madison, WI, USA) on a GLO-MAX 20/20 luminometer (Promega) after culturing the protoplasts under low light conditions for 16 h. The LUC/REN ratio is an indicator of transcriptional activity.

ChIP assays

An HA-coding sequence was fused in-frame to the 3′ end of the *CDF4* gene, and the gene fusion was subcloned into the pER8 vector. The expression construct was then transformed into Col-0 plants. Two- or five-week-old pER8::*CDF4*::HA transgenic plants were grown on MS agar plates and those that expressed CDF4::HA *via* induction by estradiol for a period were used to conduct ChIP experiments according to a previously described method using anti-HA polyclonal antibodies (Roche:118674231) [48, 84]. The qRT–PCR primers used are listed in Appendix Table S3.

Recombinant protein purification

The full-length CDF4 CDS was cloned into the pET30a and pET41b vectors and transformed into *Escherichia coli*. The recombinant protein was induced at 16°C and purified in its native form using Qiagen Ni-NTA agarose (Limburg, The Netherlands) following the manufacturer's protocol.

EMSA

Construction of plasmid for the expression of recombinant CDF4 protein in *E. coli* and purification of CDF4 protein were conducted. A standard binding reaction was performed in a total volume of 10 μl by incubation of an appropriate amount of purified CDF4 protein with 10 fm of biotin-labeled probe DNA and 1 μg poly (dI-dC) in buffer (25 mM HEPES-potassium hydroxide, pH 7.5, 100 mM KCl, 0.1 mM EDTA, 10% [v/v] glycerol, 1 mM DTT) at room temperature for 30 min. The binding reaction products were resolved on the 6% polyacrylamide gel run in 0.5 × TBE. The probes for EMSA are described in Appendix Table S3.

DNA–protein interaction ELISA

DNA–protein interaction enzyme-linked immunosorbent assay (DPI-ELISA) was performed as described in Brand *et al* [85]. Full-length glutathione S-transferase (GST)-CDF4 protein was produced in the BL21 strain and purified using Glutathione Superflow Resin (Qiagen). An antibody against GST conjugated with horseradish peroxidase (HRP) was used to detect the bound proteins.

Scanning electron microscopy

The leaves were cut and sputter-coated with gold and visualized using a Hitachi JEOL JSM-6360LV SEM (scanning electron microscope).

Analysis of catalase enzymatic activity

The catalase activity assay was performed using a catalase assay kit (Beyotime Biotechnology). Briefly, samples were frozen in liquid nitrogen and fully ground into a powder; each sample was suspended in 100 μl extraction buffer (10 mM Tris–HCl, pH 7.6, 150 mM NaCl, and 1% Nonidet P-40) and centrifuged at 12,000 rpm for 12 min at 4°C. The supernatant was used to analyze catalase activity. Catalase activity is presented as units/mg protein. One unit of catalase activity represents the amount of enzyme that catalyzes the decomposition of 1 μM H_2O_2 per minute at 25°C. Protein concentration was measured using a BCA protein assay kit (Beyotime Biotechnology).

Statistical analysis and multiple alignments

Student's *t*-test or ANOVA was carried out, and differences were considered significant when $P < 0.05$. Multiple alignments of the predicted amino acid sequences and phylogenetic analysis were performed using DNA MAN 6.0 and MEGA 4.1 software.

Expanded View for this article is available online.

Acknowledgements

This work was supported by the National Natural Science Foundation of China (Grant Nos. 31500236, U1738107, 31600684, 31971172, and 31570859), the Strategic Priority Research Program of the Chinese Academy of Sciences (Grant Nos. XDA04020202-15 and XDA04020415), and the China Manned Space Flight Technology Project.

Author contributions

PX and WC conceived and designed the research. PX wrote the article with help from WC. PX conducted the experiments and contributed to the study design with help from HY. All authors approved the final draft of the manuscript and agreed to its submission.

Conflict of interest

The authors declare that they have no conflict of interest.

References

1. Nam HG (1997) The molecular genetic analysis of leaf senescence. *Curr Opin Biotechnol* 8: 200 – 207
2. Quirino BF, Noh YS, Himelblau E, Amasino RM (2000) Molecular aspects of leaf senescence. *Trends Plant Sci* 5: 278 – 282
3. Lim PO, Kim HJ, Nam HG (2007) Leaf senescence. *Annu Rev Plant Biol* 58: 115 – 136
4. Aharoni N, Back A, Benyehoshua S, Richmond AE (1975) Exogenous gibberellic-acid and cytokinin isopentenyladenine retardants of senescence in romaine lettuce. *J Am Soc Hortic Sci* 100: 4 – 6
5. Gan S, Amasino RM (1995) Inhibition of leaf senescence by autoregulated production of cytokinin. *Science* 270: 1986 – 1988
6. Yu K, Wei J, Ma Q, Yu D, Li J (2009) Senescence of aerial parts is impeded by exogenous gibberellic acid in herbaceous perennial *Paris polyphylla*. *J Plant Physiol* 166: 819 – 830
7. Kim JI, Murphy AS, Baek D, Lee SW, Yun DJ, Bressan RA, Narasimhan ML (2011) YUCCA6 over-expression demonstrates auxin function in delaying leaf senescence in *Arabidopsis thaliana*. *J Exp Bot* 62: 3981 – 3992
8. Zacarias L, Reid MS (1990) Role of growth-regulators in the senescence of *Arabidopsis-Thaliana* leaves. *Physiol Plantarum* 80: 549 – 554
9. Reid MS, Wu MJ (1992) Ethylene and flower senescence. *Plant Growth Regul* 11: 37 – 43
10. Breeze E, Harrison E, McHattie S, Hughes L, Hickman R, Hill C, Kiddle S, Kim YS, Penfold CA, Jenkins D *et al* (2011) High-resolution temporal profiling of transcripts during *Arabidopsis* leaf senescence reveals a distinct chronology of processes and regulation. *Plant Cell* 23: 873 – 894
11. Van der Graaff E, Schwacke R, Schneider A, Desimone M, Flugge UI, Kunze R (2006) Transcription analysis of *Arabidopsis* membrane transporters and hormone pathways during developmental and induced leaf senescence. *Plant Physiol* 141: 776 – 792
12. Nambara E, Marion-Poll A (2005) Abscisic acid biosynthesis and catabolism. *Annu Rev Plant Biol* 56: 165 – 185
13. Schwartz SH, Tan BC, McCarty DR, Welch W, Zeevaart JA (2003) Substrate specificity and kinetics for VP14, a carotenoid cleavage dioxygenase in the ABA biosynthetic pathway. *Biochim Biophys Acta* 1619: 9 – 14
14. Bittner F, Oreb M, Mendel RR (2001) ABA3 is a molybdenum cofactor sulfurase required for activation of aldehyde oxidase and xanthine dehydrogenase in *Arabidopsis thaliana*. *J Biol Chem* 276: 40381 – 40384
15. Yang J, Worley E, Udvardi M (2014a) A NAP-AAO3 regulatory module promotes chlorophyll degradation via ABA biosynthesis in *Arabidopsis* leaves. *Plant Cell* 26: 4862 – 4874
16. Jensen MK, Lindemose S, De Masi F, Reimer JJ, Nielsen ML, Perera V, Chris T, Franziska T, Murray R, Mundy J *et al* (2013) ATAF1 transcription factor directly regulates abscisic acid biosynthetic gene NCED3 in *Arabidopsis thaliana*. *FEBS Open Bio* 3: 321 – 327
17. Weiner JJ, Peterson FC, Volkman BF, Cutler SR (2010) Structural and functional insights into core ABA signaling. *Curr Opin Plant Biol* 13: 495 – 502
18. Melcher K, Xu Y, Ng LM, Zhou XE, Soon FF, Chinnusamy V, Suino-Powell KM, Kovach A, Tham FS, Cutler SR *et al* (2010) Identification and mechanism of ABA receptor antagonism. *Nat Struct Mol Biol* 17: 1102 – 1108
19. Jing HC, Dijkwel PP (2008) CPR5: a Jack of all trades in plants. *Plant Signal Behav* 3: 562 – 563
20. Jing HC, Hebeler R, Oeljeklaus S, Sitek B, Stuhler K, Meyer HE, Sturre MJ, Hille J, Warscheid B, Dijkwel PP (2008) Early leaf senescence is associated with an altered cellular redox balance in *Arabidopsis* cpr5/old1 mutants. *Plant Biol (Stuttg)* 10(Suppl 1): 85 – 98

21. Shahnejatbushehri S, Tarkowska D, Sakuraba Y, Balazadeh S (2016) *Arabidopsis* NAC transcription factor JUB1 regulates GA/BR metabolism and signalling. *Nat Plants* 2: 16013
22. Lee S, Seo PJ, Lee HJ, Park CM (2012) A NAC transcription factor NTL4 promotes reactive oxygen species production during drought-induced leaf senescence in *Arabidopsis*. *Plant J* 70: 831 – 844
23. Shi WL, Jia WS, Liu X, Zhang SQ (2004) Protein tyrosine phosphatases involved in signaling of the ABA-induced H_2O_2 generation in guard cells of Vicia faba L. *Chinese Sci Bull* 49: 1841 – 1846
24. Kwak JM, Mori IC, Pei ZM, Leonhardt N, Torres MA, Dangl JL, Bloom RE, Bodde S, Jones JD, Schroeder JI (2003) NADPH oxidase AtrbohD and AtrbohF genes function in ROS-dependent ABA signaling in *Arabidopsis*. *EMBO J* 22: 2623 – 2633
25. Yu YL, Zhen SM, Wang S, Wang YP, Cao H, Zhang YZ, Li JR, Yan YM (2016) Comparative transcriptome analysis of wheat embryo and endosperm responses to ABA and H_2O_2 stresses during seed germination. *BMC Genom* 17: 97
26. Zentgraf U, Jobst J, Kolb D, Rentsch D (2004) Senescence-related gene expression profiles of rosette leaves of *Arabidopsis thaliana*: leaf age versus plant age. *Plant Biol (Stuttg)* 6: 178 – 183
27. Balazadeh S, Riano-Pachon DM, Mueller-Roeber B (2008a) Transcription factors regulating leaf senescence in *Arabidopsis thaliana*. *Plant Biol (Stuttg)* 10(Suppl 1): 63 – 75
28. Balazadeh S, Parlitz S, Mueller-Roeber B, Meyer RC (2008b) Natural developmental variations in leaf and plant senescence in *Arabidopsis thaliana*. *Plant Biol (Stuttg)* 10(Suppl 1): 136 – 147
29. Miao Y, Zentgraf U (2007) The antagonist function of *Arabidopsis* WRKY53 and ESR/ESP in leaf senescence is modulated by the jasmonic and salicylic acid equilibrium. *Plant Cell* 19: 819 – 830
30. Huang Y, Feng CZ, Ye Q, Wu WH, Chen YF (2016) *Arabidopsis* WRKY6 transcription factor acts as a positive regulator of abscisic acid signaling during seed germination and early seedling development. *PLoS Genet* 12: e1005833
31. Balazadeh S, Kwasniewski M, Caldana C, Mehrnia M, Zanor MI, Xue GP, Mueller-Roeber B (2011) ORS1, an H(2)O(2)-responsive NAC transcription factor, controls senescence in *Arabidopsis thaliana*. *Mol Plant* 4: 346 – 360
32. Kou X, Watkins CB, Gan SS (2012) *Arabidopsis* AtNAP regulates fruit senescence. *J Exp Bot* 63: 6139 – 6147
33. Li Z, Peng J, Wen X, Guo H (2013) Ethylene-insensitive3 is a senescence-associated gene that accelerates age-dependent leaf senescence by directly repressing mir164 transcription in *Arabidopsis*. *Plant Cell* 25: 3311 – 3328
34. Balazadeh S, Siddiqui H, Allu AD, Matallana-Ramirez LP, Caldana C, Mehrnia M, Zanor MI, Kohler B, Mueller-Roeber B (2010) A gene regulatory network controlled by the NAC transcription factor ANAC092/AtNAC2/ORE1 during salt-promoted senescence. *Plant J* 62: 250 – 264
35. Yang SD, Seo PJ, Yoon HK, Park CM (2011) The *Arabidopsis* NAC transcription factor VNI2 integrates abscisic acid signals into leaf senescence via the COR/RD genes. *Plant Cell* 23: 2155 – 2168
36. Shahnejat-Bushehri S, Nobmann B, Devi Allu A, Balazadeh S (2016) JUB1 suppresses *Pseudomonas syringae*-induced defense responses through accumulation of DELLA proteins. *Plant Signal Behav* 11: e1181245
37. Kim YS, Sakuraba Y, Han SH, Yoo SC, Paek NC (2013) Mutation of the *Arabidopsis* NAC016 transcription factor delays leaf senescence. *Plant Cell Physiol* 54: 1660 – 1672
38. Sakuraba Y, Jeong J, Kang MY, Kim J, Paek NC, Choi G (2014) Phytochrome-interacting transcription factors PIF4 and PIF5 induce leaf senescence in *Arabidopsis*. *Nat Commun* 5: 4636
39. Roberts JA, Elliott KA, Gonzalez-Carranza ZH (2002) Abscission, dehiscence, and other cell separation processes. *Annu Rev Plant Biol* 53: 131 – 158
40. Del Campillo E (1999) Multiple endo-1,4-beta-D-glucanase (cellulase) genes in *Arabidopsis*. *Curr Top Dev Biol* 46: 39 – 61
41. Cho HT, Cosgrove DJ (2000) Altered expression of expansin modulates leaf growth and pedicel abscission in *Arabidopsis thaliana*. *Proc Natl Acad Sci USA* 97: 9783 – 9788
42. Butenko MA, Patterson SE, Grini PE, Stenvik GE, Amundsen SS, Mandal A, Aalen RB (2003) Inflorescence deficient in abscission controls floral organ abscission in *Arabidopsis* and identifies a novel family of putative ligands in plants. *Plant Cell* 15: 2296 – 2307
43. Stenvik GE, Tandstad NM, Guo Y, Shi CL, Kristiansen W, Holmgren A, Clark SE, Aalen RB, Butenko MA (2008) The EPIP peptide of inflorescence deficient in abscission is sufficient to induce abscission in *Arabidopsis* through the receptor-like kinases haesa and haesa-like2. *Plant Cell* 20: 1805 – 1817
44. Fang SC, Fernandez DE (2002) Effect of regulated overexpression of the MADS domain factor AGL15 on flower senescence and fruit maturation. *Plant Physiol* 130: 78 – 89
45. Cai S, Lashbrook CC (2008) Stamen abscission zone transcriptome profiling reveals new candidates for abscission control: enhanced retention of floral organs in transgenic plants overexpressing *Arabidopsis* zinc finger protein2. *Plant Physiol* 146: 1305 – 1321
46. Wei PC, Tan F, Gao XQ, Zhang XQ, Wang GQ, Xu H, Li LJ, Chen J, Wang XC (2010) Overexpression of AtDOF4.7, an *Arabidopsis* DOF family transcription factor, induces floral organ abscission deficiency in *Arabidopsis*. *Plant Physiol* 153: 1031 – 1045
47. Yanagisawa S (2002) The Dof family of plant transcription factors. *Trends Plant Sci* 7: 555 – 560
48. Xu P, Chen H, Ying L, Cai W (2016) AtDOF5.4/OBP4, a DOF transcription factor gene that negatively regulates cell cycle progression and cell expansion in *Arabidopsis thaliana*. *Sci Rep* 6: 27705
49. Papi M, Sabatini S, Altamura MM, Hennig L, Schafer E, Costantino P, Vittorioso P (2002) Inactivation of the phloem-specific Dof zinc finger gene DAG1 affects response to light and integrity of the testa of *Arabidopsis* seeds. *Plant Physiol* 128: 411 – 417
50. Ward JM, Cufr CA, Denzel MA, Neff MM (2005) The Dof transcription factor OBP3 modulates phytochrome and cryptochrome signaling in *Arabidopsis*. *Plant Cell* 17: 475 – 485
51. Skirycz A, Reichelt M, Burow M, Birkemeyer C, Rolcik J, Kopka J, Zanor MI, Gershenzon J, Strnad M, Szopa J *et al* (2006) DOF transcription factor AtDof1.1 (OBP2) is part of a regulatory network controlling glucosinolate biosynthesis in *Arabidopsis*. *Plant J* 47: 10 – 24
52. Park DH, Lim PO, Kim JS, Cho DS, Hong SH, Nam HG (2003) The *Arabidopsis* COG1 gene encodes a Dof domain transcription factor and negatively regulates phytochrome signaling. *Plant J* 34: 161 – 171
53. Negi J, Moriwaki K, Konishi M, Yokoyama R, Nakano T, Kusumi K, Hashimoto-Sugimoto M, Schroeder JI, Nishitani K, Yanagisawa S *et al* (2013) A Dof transcription factor, SCAP1, is essential for the development of functional stomata in *Arabidopsis*. *Curr Biol* 23: 479 – 484
54. Guo Y, Qin G, Gu H, Qu LJ (2009) Dof5.6/HCA2, a Dof transcription factor gene, regulates interfascicular cambium formation and vascular tissue development in *Arabidopsis*. *Plant Cell* 21: 3518 – 3534
55. Kim HS, Kim SJ, Abbasi N, Bressan RA, Yun DJ, Yoo SD, Kwon SY, Choi SB (2010) The DOF transcription factor Dof5.1 influences leaf axial patterning by promoting Revoluta transcription in *Arabidopsis*. *Plant J* 64: 524 – 535

56. Gardiner J, Sherr I, Scarpella E (2010) Expression of DOF genes identifies early stages of vascular development in *Arabidopsis* leaves. *Int J Dev Biol* 54: 1389 – 1396
57. Goralogia GS, Liu TK, Zhao L, Panipinto PM, Groover ED, Bains YS, Imaizumi T (2017) CYCLING DOF FACTOR 1 represses transcription through the topless co-repressor to control photoperiodic flowering in *Arabidopsis*. *Plant J* 92: 244 – 262
58. Corrales AR, Carrillo L, Lasierra P, Nebauer SG, Dominguez-Figueroa J, Renau-Morata B, Pollmann S, Granell A, Molina RV, Vicente-Carbajosa J *et al* (2017) Multifaceted role of cycling DOF factor 3 (CDF3) in the regulation of flowering time and abiotic stress responses in *Arabidopsis*. *Plant Cell Environ* 40: 748 – 764
59. Fornara F, Panigrahi KC, Gissot L, Sauerbrunn N, Ruhl M, Jarillo JA, Coupland G (2009) *Arabidopsis* DOF transcription factors act redundantly to reduce constans expression and are essential for a photoperiodic flowering response. *Dev Cell* 17: 75 – 86
60. Henriques R, Wang H, Liu J, Boix M, Huang LF, Chua NH (2017) The antiphasic regulatory module comprising CDF5 and its antisense RNA FLORE links the circadian clock to photoperiodic flowering. *New Phytol* 216: 854 – 867
61. Sun Z, Guo T, Liu Y, Liu Q, Fang Y (2015) The roles of *Arabidopsis* CDF2 in transcriptional and posttranscriptional regulation of primary microRNAs. *PLoS Genet* 11: e1005598
62. Imaizumi T, Schultz TF, Harmon F, Ho LA, Kay SA (2005) FKF1 F-box protein mediates cyclic degradation of a repressor of CONSTANS in *Arabidopsis*. *Science* 309: 293 – 297
63. Pi L, Aichinger E, van der Graaff E, Llavata-Peris CI, Weijers D, Hennig L, Groot E, Laux T (2015) Organizer-derived WOX5 signal maintains root columella stem cells through chromatin-mediated repression of CDF4 expression. *Dev Cell* 33: 576 – 588
64. Schwartz SH, Leon-Kloosterziel KM, Koornneef M, Zeevaart JA (1997) Biochemical characterization of the aba2 and aba3 mutants in *Arabidopsis thaliana*. *Plant Physiol* 114: 161 – 166
65. Krebs J, Mueller-Roeber B, Ruzicic S (2010) A novel bipartite nuclear localization signal with an atypically long linker in DOF transcription factors. *J Plant Physiol* 167: 583 – 586
66. Lashbrook CC, Klee HJ (1999) Ethylene regulation of abscission competence. In *Biology and biotechnology of the plant hormone ethylene II*, Kanellis AK, Chang C, Klee H, Bleecker AB, Pech JC, Grierson D (eds), pp 227 – 233. Dordrecht: Springer
67. Ogawa M, Kay P, Wilson S, Swain SM (2009) *Arabidopsis* dehiscence zone polygalacturonase1 (adpg1), adpg2, and quartet2 are polygalacturonases required for cell separation during reproductive development in *Arabidopsis*. *Plant Cell* 21: 216 – 233
68. Sawicki M, Ait Barka E, Clement C, Vaillant-Gaveau N, Jacquard C (2015) Cross-talk between environmental stresses and plant metabolism during reproductive organ abscission. *J Exp Bot* 66: 1707 – 1719
69. Riefler M, Novak O, Strnad M, Schmu T (2006) *Arabidopsis* cytokinin receptor mutants reveal functions in shoot growth, leaf senescence, seed size, germination, root development, and cytokinin metabolism. *Plant Cell* 18: 40 – 54
70. Raines T, Shanks C, Cheng CY, McPherson D, Argueso CT, Kim HJ, Franco-Zorrilla JM, López-Vidriero I, Solano R, Vaňková R *et al* (2016) The cytokinin response factors modulate root and shoot growth and promote leaf senescence in *Arabidopsis*. *Plant Journal* 85: 134 – 147
71. Lim PO, Lee IC, Kim J, Kim HJ, Ryu JS, Woo HR, Nam HG (2010) Auxin response factor 2 (arf2) plays a major role in regulating auxin-mediated leaf longevity. *J Exp Bot* 61: 1419 – 1430
72. Zhang S, Li C, Wang R, Chen Y, Shu S, Huang R, Zhang D, Li J, Xiao S, Yao N *et al* (2017) The *Arabidopsis* mitochondrial protease FtSH4 is involved in leaf senescence via regulation of WRKY-dependent salicylic acid accumulation and signaling. *Plant Physiol* 173: 2294 – 2307
73. Besseau S, Li J, Palva ET (2012) WRKY54 and WRKY70 co-operate as negative regulators of leaf senescence in *Arabidopsis thaliana*. *J Exp Bot* 63: 2667 – 2679
74. Yang L, Zhang J, He J, Qin Y, Hua D, Duan Y, Chen Z, Gong Z (2014b) ABA-mediated ROS in mitochondria regulate root meristem activity by controlling PLETHORA expression in *Arabidopsis*. *PLoS Genet* 10: e1004791
75. Mittler R, Blumwald E (2015) The roles of ROS and ABA in systemic acquired acclimation. *Plant Cell* 27: 64 – 70
76. Wu A, Allu AD, Garapati P, Siddiqui H, Dortay H, Zanor M-I, Asensi-Fabado M, Munné-Bosch S, Antonio A, Tohge T *et al* (2012) JUNGBRUNNEN1, a reactive oxygen species-responsive NAC transcription factor, regulates longevity in *Arabidopsis*. *Plant Cell* 24: 482 – 506
77. Qi W, Zhang L, Feng W, Xu H, Wang L, Jiao Z (2015) ROS and ABA signaling are involved in the growth stimulation induced by low-dose gamma irradiation in *Arabidopsis* seedling. *Appl Biochem Biotechnol* 175: 1490 – 1506
78. Watkins JM, Chapman JM, Muday GK (2017) Abscisic acid-induced reactive oxygen species are modulated by flavonols to control stomata aperture. *Plant Physiol* 175: 1807 – 1825
79. Bleecker AB, Patterson SE (1997) Last exit: senescence, abscission, and meristem arrest in *Arabidopsis*. *Plant Cell* 9: 1169 – 1179
80. Smykowski A, Zimmermann P, Zentgraf U (2010) G-Box binding factor1 reduces CATALASE2 expression and regulates the onset of leaf senescence in *Arabidopsis*. *Plant Physiol* 153: 1321 – 1331
81. Guo P, Li Z, Huang P, Li B, Fang S, Chu J, Guo H (2017) A tripartite amplification loop involving the transcription factor WRKY75, salicylic acid, and reactive oxygen species accelerates leaf senescence. *Plant Cell* 29: 2854 – 2870
82. Seo M, Peeters AJ, Koiwai H, Oritani T, Marion-Poll A, Zeevaart JA, Koornneef M, Kamiya Y, Koshiba T (2000) The *Arabidopsis* aldehyde oxidase 3 (AAO3) gene product catalyzes the final step in abscisic acid biosynthesis in leaves. *Proc Natl Acad Sci USA* 97: 12908 – 12913
83. Mustilli AC, Merlot S, Vavasseur A, Fenzi F, Giraudat J (2002) *Arabidopsis* ost1 protein kinase mediates the regulation of stomatal aperture by abscisic acid and acts upstream of reactive oxygen species production. *Plant Cell* 14: 3089 – 3099
84. Xu P, Cai W (2019) Nitrate-responsive OBP4-XTH9 regulatory module controls lateral root development in *Arabidopsis thaliana*. *PLoS Genet* 15: e1008465
85. Brand LH, Kirchler T, Hummel S, Chaban C, Wanke D (2010) DPI-ELISA: a fast and versatile method to specify the binding of plant transcription factors to DNA in vitro. *Plant Methods* 6.1: 25 – 25

